

Title: Characterization of a Selective, Reversible Inhibitor of Lysophospholipase 2 (LYPLA2)

Authors: Alexander Adibekian*, Brent R Martin*, Jae Won Chang*, Ku-Lung Hsu*, Katsunori Tsuboi*, Daniel A Bachovchin*, Anna E Speers*, Steven J Brown*, Timothy Spicer[†], Virneliz Fernandez-Vega[†], Jill Ferguson*, Benjamin F Cravatt*, Peter Hodder[†], and Hugh Rosen*

*The Scripps Research Institute, La Jolla CA; [†]The Scripps Research Institute, Jupiter, FL
Corresponding author: hrosen@scripps.edu

Assigned Assay Grant #: 1 R01 CA132630

Screening Center Name & PI: The Scripps Research Institute Molecular Screening Center (SRIMSC), H Rosen

Chemistry Center Name & PI: SRIMSC, H Rosen

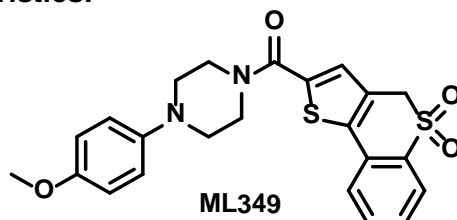
Assay Submitter & Institution: BF Cravatt, TSRI, La Jolla

PubChem Summary Bioassay Identifier (AID): 2203

Abstract:

Protein palmitoylation is an essential post-translational modification necessary for trafficking and localization of regulatory proteins that play key roles in cell growth and signaling. Multiple oncogenes, including HRAS and SRC, require palmitoylation for malignant transformation. Lysophospholipase 1 (LYPLA1) has been identified as a candidate protein palmitoyl thioesterase responsible for HRAS depalmitoylation in mammalian cells. LYPLA1 has a close homolog, LYPLA2 (65% sequence identity), whose substrate specificity and biochemical roles are, as yet, uncharacterized. Seeking chemical tools to investigate biochemical pathway involvement and potential roles in cancer pathogenesis of these enzymes, we conducted a fluorescence polarization-based competitive activity-based protein profiling (fluopol-ABPP) HTS campaign to identify inhibitors of LYPLA1 and LYPLA2. HTS identified a lead triazole urea micromolar inhibitor, which we optimized as dual LYPLA1/LYPLA2 inhibitor ML211, and reversible compounds ML348 and ML349 that act as selective LYPLA1 and LYPLA2 inhibitors, respectively. Using an advanced competitive ABPP strategy employing ABPP probes with controlled reactivity rates, we successfully confirmed potent and selective target engagement of these reversible compounds in living systems as detailed here for ML349 and in the accompanying ML348 Probe Report. Together, these compounds should greatly aid investigations into the biological function of LYPLA1 and LYPLA2.

Probe Structure & Characteristics:



CID/ML#	Target Name	IC50 (nM) [SID, AID]	Anti-target Name(s)	IC50 (nM) [SID, AID]	Fold Selective [†]	Secondary Assay(s) Name: IC50 (nM) [SID, AID]
CID 3238952/ML349	LYPLA2	144 [SID 160654496, AID 651990]	LYPLA1	> 3000 [SID 160654496, AID 651990]	> 20	Inhibition Assay, HTS hits: [SID 160654495, AID 652029] Selectivity Assay, HTS hits: [SID 160654495, AID 652030] Inhibition and Selectivity Assay SAR: [SID 160654495, AIDs 651988 and 652018] Gel-based ABPP IC50 Assay: 144 nM [SID 160654496, AID 651990] Substrate Kinetic Analysis Assay: IC50 510 nM, Ki 230 nM [SID 160654496, AIDs 652001 and 652003] In Situ Assay: [SID 160654496, AID 651986] In Vivo Assay: [SID 160654496, AID 651985] Cytox assay: [SID 160654496, AID 651991] Gel filtration assay: [SID 160654496, AID 651987] ABPP-SILAC assay: [SID 160654496, AIDs 651981 (<i>in vitro</i>), 651980 (<i>in situ</i>)]
			> 20 SHs*	> 10,000 [SID 160654495, AID 651988]**	> 69	

*As assessed by gel-based competitive ABPP in a soluble proteome derived from HEK293T cells with the serine hydrolase-specific activity-based probe FP-PEG-Rhodamine.

**IC50 of the anti-target is defined as greater than the test compound concentration at which less than or equal to 50% inhibition of the anti-target is observed; as reported in AID 651988, there were no observed anti-targets at the highest test concentration (10,000 nM) so the IC50 is reported as > 10,000 nM.

[†]Fold-selectivity was calculated as: > IC50 for anti-target/IC50 for target.

Recommendations for scientific use of the probe:

Protein palmitoylation is an essential post-translational modification (PTM), and identification of enzymes responsible for the dynamic modulation of palmitoylation is paramount to understanding its patho/physiological roles. LYPLA2 is an uncharacterized protein with high sequence similarity to LYPLA1, a serine hydrolase (SH) that we [1] and others [2] have identified as a putative protein palmitoyl thioesterase capable of regulating HRAS palmitoylation in mammalian cells. A principle goal of post-genomic research is the determination of the molecular and cellular roles of uncharacterized enzymes, like LYPLA2, through the development of selective, *in vivo*-active chemical tools. The probe described herein, ML349, can selectively inhibit LYPLA1 *in vitro* (complex proteome lysates), *in situ* (cells in culture), and *in vivo* (mouse animal models). Along with the dual LYPLA1/LYPLA2 probe ML211 and LYPLA1-selective probe ML348 (see respective Probe Reports), ML349 is intended for use in primary research studies aimed at elucidating the patho/physiological roles of the LYPLA2 and LYPLA1 in living systems.



1 Introduction

Protein palmitoylation is an essential PTM necessary for trafficking and localization of regulatory proteins that play key roles in cell growth and signaling. Numerous proteins have been identified as targets of palmitoylation, including cytoskeletal proteins, kinases, receptors, and other proteins involved in various aspects of cellular signaling and homeostasis [3]. Using a global chemo-proteomic method for the metabolic incorporation and identification of palmitoylated proteins, we have been able to identify hundreds of palmitoylated proteins, revealing palmitoylation as a widespread PTM [1]. Palmitoylation involves an acyl-thioester linkage to specific cysteines [4, 5]. Given the labile properties of thioesters, palmitoylation is potentially reversible and may be regulated in a manner analogous to other PTMs (e.g., phosphorylation). As such, identification of proteins responsible for the dynamic modulation of palmitoylation is paramount to understanding its patho/physiological roles. For example, multiple oncogenes, including HRAS and SRC, require palmitoylation-mediated localization for signaling and subsequent malignant transformation [6]. It has been suggested by Waldmann *et al.* that preventing depalmitoylation of RAS by inhibiting thioesterase activity may disrupt targeted distribution (e.g., to Golgi), thereby downregulating oncogenic signaling [2]. This suggests that inhibitors of protein palmitoyl thioesterases may act as tumor suppressors by preventing aberrant growth signaling. More than a decade ago, the cytosolic serine hydrolase (SH) acyl-protein thioesterase 1 (APT1) was identified as an *in vitro* HRAS palmitoyl thioesterase [7]. Initially classified as lysophospholipase 1 (LYPLA1) [8], the enzyme has since been demonstrated to have several hundred-fold higher activity as a protein palmitoyl thioesterase. While the *in vitro* data [7, 9] provided an intriguing clue to its possible role *in vivo*, much less is known about the *in vivo* thioesterase activity of LYPLA1. LYPLA2 (a.k.a. APT2) is 65% identical to LYPLA1, and also exhibits lysophospholipase activity *in vitro*, but its potential role as a thioesterase is unknown [10]. shRNA knockdown studies of LYPLA2 revealed only partial knockdown of the enzyme, making substrate identification inconclusive (unpublished). A principle goal of post-genomic research is the determination of the molecular and cellular role of uncharacterized enzymes like LYPLA1 and LYPLA2. Small molecule inhibitors would be of particular utility when combined with global methods for profiling dynamic palmitoylation [1, 11] for investigation of LYPLA1/LYPLA2 biology.

Following a MLPCN HTS inhibitor discovery campaign (AIDs 2174, 2177, 2232, and 2233), we previously reported a LYPLA1/LYPLA2 dual inhibitor, ML211, based on an irreversible triazole urea scaffold. In the same screen, we also identified reversible compounds ML349 and ML348 that showed high selectivity for LYPLA2 and LYPLA1, respectively [12].

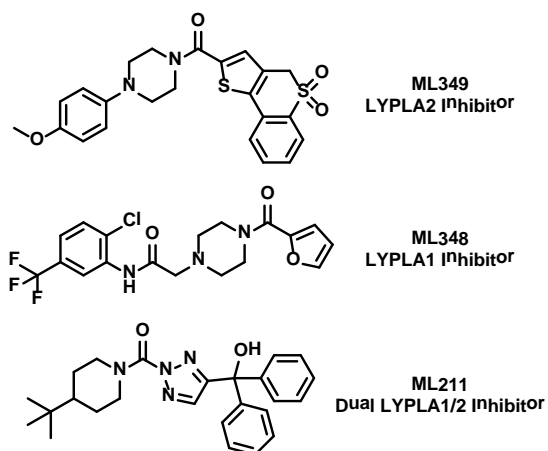


Figure 1-1. Structures of LYPLA2 and LYPLA1 Probes derived from HTS at SRIMSC. See respective Probe Reports for ML211 and ML348 for more details.

Several inhibitors of LYPLA1 have been described [2, 13, 14] (see **Section 4.1** for structures and further discussion), but none of these agents have proven capable of selectively inhibiting LYPLA1 activity in living systems, and no selective inhibitors of LYPLA2 have been reported to date. To comprehensively identify LYPLA1 and LYPLA2 substrates and functionally test the role of these enzymes in dynamic palmitoylation and tumorigenesis, development of high affinity and selective inhibitors capable of achieving temporal and more complete control over activity is critical.

As SHs, catalytically active LYPLA1 and LYPLA2 are readily labeled by fluorescent activity-based protein profiling (ABPP) probes bearing a fluorophosphonate (FP) reactive group [15]. This reactivity can be exploited for inhibitor discovery using a competitive-ABPP platform, whereby small molecule enzyme inhibition is assessed by the ability to out-compete ABPP probe labeling [16]. Competitive ABPP has also been configured to operate in a high-throughput manner via fluorescence polarization readout, fluopol-ABPP [17]. In conjunction with the SRIMSC, we applied fluopol-ABPP to LYPLA1 and LYPLA2 inhibitor discovery. As mentioned above, initial efforts focused on deriving a dual LYPLA1/2 inhibitor based on a triazole urea scaffold. The probe ML211 inhibits both target enzymes with low nanomolar potency and is active *in situ*. Because ML211 operated by an irreversible mechanism, confirming target engagement in living systems was a comparatively straightforward process using a competitive ABPP strategy. However, the analogous characterization of reversible compounds is typically a more challenging endeavor. As such, to fully characterize the reversible probes ML349 and ML348, we utilized kinetically-tuned, *in vivo*-active ABPP probes that allowed direct profiling of reversible inhibitors. By controlling reactivity rates, these ABPP probes minimized false negative results from inhibitors outcompeting ABPP probe labeling, thus enhancing detection of target (and anti-target) engagement [12]. As detailed herein, ML349 is highly potent against LYPLA2 (IC₅₀ of 144 nM *in vitro*) and is the first reported selective LYPLA2 inhibitor. ML349 exhibited high selectivity (>20-fold) vs. LYPLA1 and all other (~20) SHs assessed by gel-based competitive ABPP. In-depth profiling by quantitative MS-based methods confirmed selectivity among the SH superfamily, designating ML349 as a promising chemical tool for investigation of LYPLA2 biology.

2 Materials and Methods

All reagents for chemical synthesis were purchased from Sigma-Aldrich, Acros, Fisher, Fluka, ChemDiv, or Aurora and used without further purification. Dry solvents were obtained by passing commercially available pre-dried, oxygen-free formulations through activated alumina columns. All reactions were carried out under a nitrogen atmosphere using oven-dried glassware. Flash chromatography was performed using 230-400 mesh silica gel. NMR spectra were recorded on a Varian Inova-400 spectrometer and were referenced to trimethylsilane (TMS) or the residual solvent peak. Chemical shifts are reported in ppm relative to TMS and J values are reported in Hz. High resolution mass spectrometry (HRMS) experiments were performed at TSRI Mass Spectrometry Core on an Agilent mass spectrometer using electrospray ionization-time of flight (ESI-TOF). All other protocols are summarized below.

2.1 Assays

Solubility in PBS: The solubility of compounds are tested in triplicate in phosphate buffered saline (PBS), pH 7.4. per well, 198 μ l PBS is added to a Millipore Solvinert Hydrophilic PTFE 96 well filter plate: pore size: 0.45 μ m (MSRLN0450). Test compounds are introduced from 10 mM DMSO stock solutions (2 μ l). The final concentration of DMSO was 1 percent. Samples are allowed to incubate at 22 $^{\circ}$ C for 18 hours. In the morning the plate is centrifuged where the soluble portion passes through the filter and is collected in a capture plate. Clotrimazole is included as a control to assure the assay is working properly. The samples are analyzed by HPLC. Peak area is compared to a standard of known concentration. In cases when the concentration was too low for UV analysis or when the compound did not possess a good chromophore, LC-MS-MS analysis is used.

Solubility in Media: The solubility of compounds are tested in triplicate in complete media (DMEM + 10% FBS). Per well, 198 μ L PBS is added to a Millipore Solvinert Hydrophilic PTFE 96 well filter plate: pore size: 0.45 μ m (MSRLN0450). Test compounds are introduced from 10 mM DMSO stock solutions (2 μ L). The final concentration of DMSO was 1 percent. Samples are allowed to incubate at 22 $^{\circ}$ C for 18 hours. In the morning the plate is centrifuged where the soluble portion passes through the filter and is collected in a capture plate. The samples are analyzed by HPLC (Agilent 1100 with diode-array detector). Peak area is compared to a standard of known concentration. In cases when the concentration was too low for UV analysis or when the compound did not possess a good chromophore, LC-MS-MS analysis is used.

Stability in PBS: Demonstration of stability in PBS was conducted by addition of 10 μ M compound from a DMSO stock to PBS in HPLC autosampler vials. Samples are held in the HPLC autosampler at ambient temperature. At approximately 0, 1, 2, 4, 8, 24, and 48 hours the samples are injected on the HPLC. Peak area and retention time are compared between injections. Data is log transformed and represented as half-life. DMSO is added as a co-solvent as needed for solubility.

Determination of Glutathione reactivity: Compound (10 μ M) is incubated at 37 $^{\circ}$ C for 6 hours in the presence of 50 μ M freshly prepared reduced glutathione. At 0 and 6 hours the samples

are injected on the HPLC. Peak area and retention time are compared between injections. Samples are evaluated for a glutathione dependent decrease in compound concentration. DMSO is added as a co-solvent as needed for solubility.

Primary Assays

Primary uHTS assay to identify LYPLA2 inhibitors (AID 2177)

Assay Overview: The purpose of this assay was to identify compounds that act as LYPLA2 inhibitors. This assay also serves as a counterscreen for a set of previous experiments entitled, "Fluorescence polarization-based primary biochemical high throughput screening assay to identify inhibitors of Protein Phosphatase Methylesterase 1 (PME-1)" (AID 2130). This competitive activity-based protein profiling (ABPP) assay uses fluorescence polarization to investigate enzyme-substrate functional interactions based on active site-directed molecular probes [3, 15]. A serine hydrolase-specific fluorophosphonate-rhodamine (FP-Rh) probe, which broadly targets enzymes from the serine hydrolase family [14] was used to label LYPLA2 in the presence of test compounds. The reaction was excited with linear polarized light and the intensity of the emitted light was measured as the polarization value (mP). As designed, test compounds that act as LYPLA2 inhibitors will prevent LYPLA2-probe interactions, thereby increasing the proportion of free (unbound) fluorescent probe in the well, leading to low fluorescence polarization. Omission of enzyme (which gives the same result as use of a catalytically-dead enzyme) serves as a positive control. Compounds were tested at a nominal concentration of 5.9 μ M.

Protocol Summary: Prior to the start of the assay, Assay Buffer (4.0 μ L; 0.01% Pluronic acid, 50 mM Tris HCl pH 8.0, 150 mM NaCl, 1mM DTT) containing LYPLA2 protein (9.38 nM) was dispensed into 1536-well microtiter plates. Next, test compound (30 nL in DMSO) or DMSO alone (0.59% final concentration) was added to the appropriate wells and incubated for 30 minutes at 25 °C. The assay was started by dispensing FP-Rh probe (1.0 μ L of 375 nM in Assay Buffer) to all wells. Plates were centrifuged and, after 10 minutes of incubation at 25 °C, fluorescence polarization was read on a Viewlux microplate reader (PerkinElmer, Turku, Finland) using a BODIPY TMR FP filter set and a BODIPY dichroic mirror (excitation = 525 nm, emission = 598 nm). Fluorescence polarization was read for 15 seconds for each polarization plane (parallel and perpendicular). The well fluorescence polarization value (mP) was obtained via the PerkinElmer Viewlux software. **Assay Cutoff:** Compounds that inhibited LYPLA2 greater than 25.78% (mean + 3 x standard deviation) were considered active.

Confirmation uHTS assay to identify LYPLA2 inhibitors (AID 2232)

Assay Overview: The purpose of this assay was to confirm activity of compounds identified as active in the primary uHTS screen (AID 2177). In this assay, the FP-Rh probe was used to label LYPLA2 in the presence of test compounds and analyzed as described above (AID 2177). Compounds were tested in triplicate at a nominal concentration of 5.9 μ M.

Protocol Summary: The assay was performed as described above (AID 2177), except that compounds were tested in triplicate. **Assay Cutoff:** Compounds that inhibited LYPLA2 greater than 25.78% were considered active.

Secondary Assays

Inhibition of LYPLA2 by top HTS hits (AID 652029)

Assay Overview: The purpose of this assay is to determine whether test compounds can inhibit LYPLA2 in a complex proteomic lysate using a competitive activity-based proteomic profiling (ABPP) assay. In this assay, a complex proteome, containing spiked-in recombinant form of LYPLA2 is incubated with test compound followed by reaction with a serine-hydrolase-specific rhodamine-conjugated fluorophosphonate (FP-Rh) activity-based probe. The reaction products are separated by SDS-PAGE and visualized in-gel using a flatbed fluorescence scanner. The percentage activity remaining is determined by measuring the integrated optical density of the bands. As designed, test compounds that act as LYPLA2 inhibitors will prevent enzyme-probe interactions, thereby decreasing the proportion of bound fluorescent probe, giving lower fluorescence intensity in the band in the gel. Percent inhibition is calculated relative to a DMSO (no compound) control.

Protocol Summary: To soluble proteome prepared from mouse brain (1 mg/ml in DPBS) is added 20 nM purified recombinant human (rh) LYPLA2. Proteome was treated with 20 μ M test compound (1 μ L of a 50x stock in DMSO) for 30 minutes at 25 $^{\circ}$ C (50 μ L reaction volume). FP-Rh (1 μ L of 50x stock in DMSO) was added to a final concentration of 2 μ M. The reaction was incubated for 30 minutes at 25 $^{\circ}$ C, quenched with 2x SDS-PAGE loading buffer, separated by SDS-PAGE and visualized by in-gel fluorescent scanning. The percentage activity remaining was determined by measuring the integrated optical density of the target rhLYPLA2 band relative to a DMSO-only (no compound) control. **Assay Cutoff:** Compounds with greater than or equal to 50% inhibition were considered active.

Inhibition of LYPLA2 and selectivity vs. LYPLA1 of top HTS hits (AID 652030)

Assay Overview: The purpose of this assay is to determine whether test compounds can inhibit LYPLA2 in a complex proteomic lysate and assess selectivity vs. LYPLA1 using a competitive activity-based proteomic profiling (ABPP) assay. In this assay, a complex proteome, containing spiked-in recombinant form of LYPLA2 is incubated with test compound followed by reaction with a serine-hydrolase-specific rhodamine-conjugated fluorophosphonate (FP-Rh) activity-based probe. The reaction products are separated by SDS-PAGE and visualized in-gel using a flatbed fluorescence scanner. The percentage activity remaining is determined by measuring the integrated optical density of the bands. As designed, test compounds that act as LYPLA2 inhibitors will prevent enzyme-probe interactions, thereby decreasing the proportion of bound fluorescent probe, giving lower fluorescence intensity in the band in the gel. Percent inhibition is calculated relative to a DMSO (no compound) control.

Protocol Summary: To membrane proteome prepared from mouse brain (1 mg/ml in DPBS) is added 20 nM purified recombinant human (rh) LYPLA2. Proteome was treated with 10 μ M test

compound (1 μL of a 50x stock in DMSO) for 30 minutes at 25 $^{\circ}\text{C}$ (50 μL reaction volume). FP-Rh (1 μL of 50x stock in DMSO) was added to a final concentration of 2 μM . The reaction was incubated for 30 minutes at 25 $^{\circ}\text{C}$, quenched with 2x SDS-PAGE loading buffer, separated by SDS-PAGE and visualized by in-gel fluorescent scanning. The percentage activity remaining was determined by measuring the integrated optical density of the target rhLYPLA2 band relative to a DMSO-only (no compound) control. **Assay Cutoff:** Compounds with greater than or equal to 30% inhibition were considered active.

Gel-based competitive ABPP analysis of reversible (AID 651988) and triazole urea (AID 652018) SAR libraries

Assay Overview: The purpose of this assay is to determine whether powder samples of test compounds can inhibit LYPLA2 and LYPLA1 in a complex proteomic lysate and to estimate compound selectivity in a competitive activity-based protein profiling (ABPP) assay. In this assay, a complex proteome is incubated with test compound followed by reaction with the serine-hydrolase-specific rhodamine-conjugated fluorophosphonate (FP-PEG-Rh) activity-based probe. FP-PEG-Rh is similar to FP-Rh, but shows slower reaction kinetics, facilitating analysis of target inhibition by reversible compounds [12]. The reaction products are separated by SDS-PAGE and visualized in-gel using a flatbed fluorescence scanner. The percentage activity remaining is determined by measuring the integrated optical density of the bands. As designed, test compounds that act as LYPLA2 and/or LYPLA1 inhibitors will prevent enzyme-probe interactions, thereby decreasing the proportion of bound fluorescent probe, giving lower fluorescence intensity in the band in the gel. Percent inhibition is calculated relative to a DMSO (no compound) control.

Protocol Summary: Soluble proteome (50 μL of 1 mg/ml in DPBS) of HEK293T cells was treated with 300 nM, 1 μM , or 10 μM test compound (1 μL of a 50x stock in DMSO). Test compounds were incubated for 30 minutes at 37 $^{\circ}\text{C}$. FP-PEG-Rh (1 μL of 50x stock in DMSO) was added to a final concentration of 5 μM . The reaction was incubated for 30 minutes at 25 $^{\circ}\text{C}$, quenched with 2x SDS-PAGE loading buffer, separated by SDS-PAGE and visualized by in-gel fluorescent scanning. The percentage activity remaining was determined by measuring the integrated optical density of the LYPLA2 and LYPLA1 bands relative to a DMSO-only (no compound) control. From among the 20+ other distinct bands visible, anti-targets are only listed if greater than or equal to 50% inhibition is observed at any concentration tested. **Assay Cutoff:** Compounds with greater than or equal to 50% inhibition at 300 nM were considered active.

Determination of IC50 values for LYPLA2 and LYPLA1 by competitive ABPP (AID 651990)

Assay Overview: The purpose of this assay is to determine IC50 values of powder samples of test compounds for LYPLA2 and LYPLA1 in a complex proteomic lysate using a competitive activity-based protein profiling (ABPP) assay. In this assay, a complex proteome is incubated with test compound followed by reaction with the serine-hydrolase-specific rhodamine-conjugated fluorophosphonate (FP-PEG-Rh) activity-based probe. FP-PEG-Rh is similar to FP-Rh, but shows slower reaction kinetics, facilitating analysis of target inhibition by reversible compounds [12]. The reaction products are separated by SDS-PAGE and visualized in-gel using a flatbed fluorescence scanner. The percentage activity remaining is determined by

measuring the integrated optical density of the bands. As designed, test compounds that act as LYPLA2 and/or LYPLA1 inhibitors will prevent enzyme-probe interactions, thereby decreasing the proportion of bound fluorescent probe, giving lower fluorescence intensity in the band in the gel. Percent inhibition is calculated relative to a DMSO (no compound) control.

Protocol Summary: Soluble proteome (50 μ L of 1 mg/ml in DPBS) of HEK293T cells was treated with varying concentrations of test compound (1 μ L of a 50x stock in DMSO) for 30 minutes at 37 °C. FP-PEG-Rh (1 μ L of 50x stock in DMSO) was added to a final concentration of 5 μ M. The reaction was incubated for 30 minutes at 25 °C, quenched with 2x SDS-PAGE loading buffer, separated by SDS-PAGE and visualized by in-gel fluorescent scanning. The percentage activity remaining was determined by measuring the integrated optical density of the LYPLA2 and LYPLA1 bands relative to a DMSO-only (no compound) control. IC₅₀ values were determined from dose-response curves from three replicates at each inhibitor concentration: 3000 nM to 1000 nM, 300 nM to 100 nM, 30 nM, and 1 nM. **Assay Cutoff:** Compounds with an IC₅₀ less than or equal to 500 nM were considered active.

Kinetic analysis of inhibition of LYPLA2 (AID 652001) and LYPLA1 (AID 652003) by substrate assay

Assay Overview: The purpose of this assay is to determine kinetic parameters (V_{max} , K_m , K_i , and IC₅₀ values) for powder samples of test compounds that act as reversible inhibitors for LYPLA2 and LYPLA1 using a fluorogenic substrate (resorufin acetate)-based assay. To determine V_{max} and K_m values, LYPLA2 or LYPLA1 is incubated with varying concentrations of substrate and the rate of enzymatic hydrolysis (as indicated by fluorescence intensity) is monitored as a function of time. Initial velocities for each substrate concentration are determined and used to calculate V_{max} and K_m using standard Michaelis-Menten kinetics. To obtain IC₅₀ values, LYPLA2 or LYPLA1 is incubated with varying concentrations of inhibitor at a fixed substrate concentration, and fluorescence intensity is monitored as a function of time. Initial velocities determined for each inhibitor concentration are used to calculate IC₅₀ values. From these data, K_i values can be calculated using the Cheng-Prusoff equation. For all assays, enzyme activity is calculated relative to a catalytically-dead (LYPLA2- S122A or LYPLA1- S119A) enzyme control.

Protocol Summary: Substrate resorufin acetate was dissolved in DMSO. Active or catalytically-dead enzyme solutions (10 nM) were prepared in DPBS adjusted to pH 6.5 with sodium acetate and 0.2% pluronic F127. In a black-bottom half-area 96 well plate, 5 μ L of substrate was aliquoted at varying concentrations (**LYPLA2:** 200 μ M, 180 μ M, 160 μ M, 140 μ M, 100 μ M, 80 μ M, 40 μ M, 30 μ M, 20 μ M, 17.5 μ M, 15 μ M, 12.5 μ M, 10 μ M, 7.5 μ M, 5 μ M, 2.5 μ M, 0 μ M ; **LYPLA1:** 180 μ M, 140 μ M, 100 μ M, 70 μ M, 60 μ M, 50 μ M, 35 μ M, 25 μ M, 15 μ M, 7.5 μ M, 3.75 μ M, 0 μ M). The assay was initiated upon addition of enzyme (95 μ L of 10 nM) using a multi-channel pipette, and reactions quickly mixed by pipetting up and down several times. Fluorescence intensity was measured on a Tecan F500 plate reader at room temperature every 30 seconds using a 525/35 nM excitation filter, a 600/10 nM emission filter, and a 560 LP dichroic filter. Each concentration was performed as 4 separate replicates for both the active and dead enzymes. After subtracting background (average fluorescence intensity of

catalytically-dead enzyme at each time point for each assay condition), fluorescence intensity was plotted vs. time and initial velocities were calculated using standard straight-line plots (with non-linear regression) in GraphPad Prism using the first ~6 minutes of the reaction. The initial velocities (+/- SEM, plotted vs. substrate concentration) were analyzed using standard Michaelis-Menten kinetics (GraphPad Prism) to derive the Vmax and Km values. Software-generated values and SEM are reported.

To calculate the Ki values, the same experimental setup was used. Active or catalytically-dead enzyme (10 nM) was incubated with varying inhibitor concentrations (**LYPLA2**: 10 µM, 6 µM, 4 µM, 2 µM, 1 µM, 0.8 µM, 0.6 µM, 0.4 µM, 0.2 µM, 0.1 µM, 0.05 µM, 0 µM ; **LYPLA1**: 11-point 2-fold dilution series from 25 µM to 24 nM, 0 nM) for 15 minutes (95 µL total volume), and then aliquoted into 96-well plate wells containing a fixed concentration of resorufin acetate substrate (**LYPLA2**: 30 µM, 5 µL; **LYPLA1**: 50 µM, 5 µL). Fluorescence intensity was monitored as described above. After background subtraction, the initial velocities were calculated as described above, plotted vs. inhibitor concentration, and analyzed to derive IC50 values (standard one phase decay, GraphPad Prism). Software-generated values and SEM are reported. The Ki values were calculated using the Cheng-Prusoff equation. **Assay Cutoff:** Compounds with an IC50 value of less than or equal to 10 µM were considered active.

Analysis of Cytotoxicity (AID 651991)

Assay Overview: The purpose of this assay is to determine cytotoxicity of powder samples of test compounds. In this assay, HEK293T cells in either serum-free medium or medium containing fetal calf serum (FCS) are incubated with test compounds, followed by determination of cell viability. The assay utilizes the WST-1 substrate which is converted into colorimetric formazan dye by the metabolic activity of viable cells. The amount of formed formazan directly correlates to the number of metabolically active cells in the culture. As designed, compounds that reduce cell viability will result in decreased absorbance of the dye.

Protocol Summary: This assay was started by dispensing HEK293T in DMEM medium supplemented with 10% FCS (100 µL, 15,000 cells/well) into a 96-well plate. Cells were incubated for 24 hours at 37 °C in a humidified incubator, medium was removed, and 100 µL of fresh, serum-free medium or medium supplemented with 10% FCS was added. Compound (10 µL of 11x stocks in medium containing 10% DMSO) or an equal volume medium containing 10% DMSO only was added to each well. Cells were incubated for 48 hours at 37 °C in a humidified incubator and cell viability was determined by the WST-1 assay (Roche) according to manufacturer instructions. CC50 values were determined from dose-response curves from six replicates at each inhibitor concentration (50000, 10000, 2000, 400, 80, 16, and 3.2 nM). **Assay Cutoff:** Compounds with CC50 values less than or equal to 10 µM were considered active (cytotoxic).

Gel filtration to assess mode of action (AID 651987)

Assay Overview: The purpose of this assay is to determine whether powder samples of test compounds inhibit LYPLA2 and LYPLA1 in a reversible or irreversible manner. In this assay, a complex proteome is incubated with test compound and a fraction of the assay mixture is

passed over a Sephadex G-25M column before reaction with the serine-hydrolase-specific fluorophosphonate-PEG-rhodamine (FP-PEG-Rh) probe. FP-PEG-Rh is similar to FP-Rh, but shows slower reaction kinetics, facilitating analysis of target inhibition by reversible compounds [12]. The reaction products are separated by SDS-PAGE and visualized in-gel using a flatbed fluorescence scanner. The percentage activity remaining is determined by measuring the integrated optical density (IOD) of the bands relative to a DMSO (no compound) control. As designed, test compounds that act as irreversible inhibitors will prevent enzyme-probe interactions both before and after gel filtration, leading to low fluorescence intensity in the band in the gel. In contrast, compounds that act as reversible inhibitors will show recovery of probe labeling (and higher fluorescence intensity in the band in the gel) following gel filtration to remove small molecules from the sample.

Protocol Summary: Soluble proteome (2 mL of 1 mg/ml in DPBS) of HEK293T cells was treated with 10 μ M or 20 μ M test compound (50x stock in DMSO) or DMSO (control). Test compounds were incubated for 30 minutes at 37 °C. An aliquot (50 μ L) was removed from each reaction, and the remaining sample was passed over a Sephadex G-25M column 1, 2, or 3x, with an aliquot (50 μ L) set aside after each passage. Aliquot volumes were adjusted to equalize protein concentrations across all samples and reacted with FP-PEG-Rh (50x stock in DMSO; 5 μ M final concentration). The reaction was incubated for 30 minutes at 25 °C, quenched with 2x SDS-PAGE loading buffer, separated by SDS-PAGE and visualized by in-gel fluorescent scanning. The percentage activity remaining was determined by measuring the integrated optical density of the LYPLA2 and LYPLA1 bands relative to a DMSO-only (no compound) control. **Assay Cutoff:** Compounds were designated as reversible inhibitors if they exhibited greater than or equal to 50% recovery of probe labeling following gel filtration. Compounds were designated as irreversible inhibitors if they exhibited less than 50% recovery of probe labeling following gel filtration.

In situ inhibition of LYPLA2 and LYPLA1 by competitive ABPP (AID 651986)

Assay Overview: The purpose of this assay is to determine whether or not powder samples of test compounds can inhibit LYPLA2 and LYPLA1 *in situ*. In this assay, cultured HEK293T cells or BW5147-derived murine T-cells are incubated with test compound followed by the cell-permeable alkyne-functionalized triazole urea ABPP probe NHU5 [12]. NHU5 covalently reacts with a subset of serine hydrolases, including LYPLA2 and LYPLA1, and shows slower reaction kinetics than other cell-permeable serine hydrolase-specific ABPP probes (e.g., FP-alkyne), facilitating analysis of target inhibition by reversible compounds. Cells are harvested, homogenized, and reacted with a rhodamine-functionalized azide tag under copper(I)-catalyzed azide-alkyne cycloaddition (“click chemistry”) reaction conditions to allow visualization of probe-tagged proteins. The reaction products are separated by SDS-PAGE and visualized in-gel using a flatbed fluorescence scanner. The percentage activity remaining is determined by measuring the integrated optical density of the bands. As designed, test compounds that act as LYPLA2 and/or LYPLA1 inhibitors will prevent enzyme-probe interactions, thereby decreasing the proportion of bound, fluorescent-tagged probe, giving lower fluorescence intensity in the band in the gel.

Protocol Summary: HEK293T cells were grown in DMEM medium (supplemented with 10% FCS and 1x Penicillin/Streptomycin/Glutamine solution) and BW5147-derived murine T-cell hybridoma cells were grown in RPMI-1640 medium (supplemented with 10% FCS and 1x Penicillin/Streptomycin/Glutamine solution) at 37 °C in a humidified incubator (5% CO₂ atmosphere). Test compounds (5 µM final concentration) or DMSO only were directly added to the cell culture medium. After 3 hours, the cell-permeable, alkyne-functionalized probe NHU5 (50 µM final concentration) was added. After 1 hour, cells were washed (4x DPBS), harvested, isolated by centrifugation at 1,400 x g for 3 minutes, re-suspended in methanol/chloroform/dH₂O (4:1:3 v/v), and vortexed. After centrifugation at 13,000 x g for 3 minutes, the upper layer was removed and 3 volumes of methanol were added and the solution vortexed. Protein was pelleted by centrifugation at 13,000 x g for 6 minutes. The supernatant was removed and the pellet was air-dried and re-suspended in PBS by sonication. For visualization of probe-labeled proteins, click chemistry with a rhodamine-azide tag (Rh-N3; 100 µM) was carried out under standard conditions (1 mM TCEP, 100 µM TBTA ligand, 1 mM Cu(II)sulfate, 1 hour, 25 °C) to append the rhodamine fluorophore to the alkyne-functionalized NHU5 probe. Reactions were quenched with 2x SDS-PAGE loading buffer, separated by SDS-PAGE and visualized by in-gel fluorescent scanning. The percentage activity remaining was determined by measuring the integrated optical density of the bands relative to a DMSO-only (no compound) control. **Assay Cutoff:** Compounds with greater than or equal to 50% inhibition were considered active.

In vivo inhibition of LYPLA2 and LYPLA1 by competitive ABPP (AID 651985)

Assay Overview: The purpose of this assay is to determine whether or not powder samples of test compounds can inhibit LYPLA2 and LYPLA1 *in vivo*. In this assay, test compounds are administered to mice followed by the *in vivo* active alkyne-functionalized triazole urea ABPP probe NHU5 [12]. NHU5 covalently reacts with a subset of serine hydrolases, including LYPLA2 and LYPLA1, and shows slower reaction kinetics than other *in vivo* active serine hydrolase-specific ABPP probes (e.g., FP-alkyne), facilitating analysis of target inhibition by reversible compounds. Mice are sacrificed, and their tissues harvested, homogenized, and the soluble fraction isolated and reacted with a rhodamine-functionalized azide tag under copper(I)-catalyzed azide-alkyne cycloaddition (“click chemistry”) reaction conditions to allow visualization of probe-tagged proteins. The reaction products are separated by SDS-PAGE and visualized in-gel using a flatbed fluorescence scanner. The percentage activity remaining is determined by measuring the integrated optical density of the bands. As designed, test compounds that act as inhibitors will prevent enzyme-probe interactions, thereby decreasing the proportion of bound, fluorescent-tagged probe, giving lower fluorescence intensity in the band in the gel.

Protocol Summary: Test compounds were prepared as a homogeneous PEG solution by vortexing and sonicating neat compound directly into PEG300. Purpose-bred C57-black laboratory mice (<6 months old, 20–28 g) were i.p. administered with test compound (50 mg/kg; 4µL/g) or vehicle only and, after 3 hours, with NHU5 probe (PEG solution; 100 mg/kg). After 1 hour, mice were sacrificed, and tissues were removed and Dounce-homogenized directly in methanol /chloroform/dH₂O (4:1:3 v/v). After centrifugation at 13,000 x g for 3 minutes, the upper layer was removed and 3 volumes of methanol were added and solution vortexed. Protein was pelleted by centrifugation at 13,000 x g for 6 minutes. The supernatant was removed and

the pellet was air-dried and re-suspended in PBS by sonication. For visualization of probe-labeled proteins, click chemistry with a rhodamine-azide tag (Rh-N3; 100 μ M) was carried out under standard conditions (1 mM TCEP, 100 μ M TBTA ligand, 1 mM Cu(II)sulfate) to append the rhodamine fluorophore to the alkyne-functionalized NHU5 probe. Reactions were quenched with 2x SDS-PAGE loading buffer, separated by SDS-PAGE and visualized by in-gel fluorescent scanning. The percentage activity remaining was determined by measuring the integrated optical density of the bands relative to a DMSO-only (no compound) control. **Assay Cutoff:** Compounds with greater than or equal to 50% inhibition in one or more tissues tested were considered active.

Selectivity analysis by ABPP-SILAC *in vitro* (AID 651981)

Assay Overview: The purpose of this assay is to determine the selectivity profile of powder samples of test compounds using stable isotope labeling with amino acids in cell culture (SILAC) activity-based protein profiling (ABPP) *in vitro*. In this assay, cultured BW5147-derived murine T-cells are metabolically labeled with light or heavy amino acids. Cells are harvested, homogenized, and proteome fractions isolated. Light and heavy samples are treated with inhibitor and DMSO, respectively, followed by the serine-hydrolase-specific ABPP affinity probe fluorophosphonate-PEG-biotin (FP-PEG-biotin). FP-PEG-biotin is similar to FP-biotin, but shows slower reaction kinetics, facilitating analysis of target inhibition by reversible compounds. Light and heavy samples are combined in a 1:1 (w/w) ratio, and biotinylated proteins are enriched, trypsinized, and analyzed by LC/LC-MS/MS (MudPIT). Inhibition of target and anti-target activity is quantified by comparing intensities of light and heavy peptide peaks. As designed, compounds that act as inhibitors will block FP-PEG-biotin labeling, reducing enrichment in the inhibitor-treated (light) sample relative to the DMSO-treated (heavy) sample, giving a smaller light/heavy ratio for each protein. Proteins not targeted by inhibitors would be expected to have a ratio close to 1.

Sample Preparation. BW5147-derived murine T-cell hybridoma cells were initially grown for 6 passages in either light or heavy SILAC RPMI 1640 medium supplemented with 10% dialyzed FCS and 1x PenStrep Glutamine. Light medium was supplemented with 100 μ g/mL L-arginine (Sigma) and 100 μ g/mL L-lysine (Sigma). Heavy medium was supplemented with 100 μ g/mL [$^{13}\text{C}_6$ $^{15}\text{N}_4$]-L-Arginine (Isotek) and 100 μ g/mL [$^{13}\text{C}_6$ $^{15}\text{N}_2$]-L-Lysine (Isotek). Cells were harvested and homogenized by sonication in DPBS. The soluble and membrane fractions were isolated by centrifugation (100K x g, 45 minutes) and the protein concentration was adjusted to 1 mg/mL with DPBS. Membrane and soluble fractions of light cells were treated with test compound (1 μ M) and membrane and soluble fractions of heavy cells were treated with DMSO for 30 minutes at 37 $^\circ$ C. All samples were reacted with the activity-based affinity probe FP-PEG-Biotin (5 μ M) for 30 minutes at 25 $^\circ$ C. Light and heavy proteomes were mixed in 1:1 (w/w) ratio to generate one membrane and one soluble sample, which were desalted over PD-10 columns (GE Healthcare). SDS was added to a final concentration of 0.5% in 3 mL total reaction volume and biotinylated proteins were enriched on streptavidin beads (50 μ L, 1 hour, 25 $^\circ$ C). The beads were washed with 1% SDS in DPBS (1x), 6M urea (1x), and DPBS (2x), then resuspended in 6 M urea (150 μ L), reduced with 5 mM TCEP for 20 minutes, and alkylated with 10 mM iodoacetamide for 30 minutes at 25 $^\circ$ C in the dark, and urea concentration was reduced to 2 M

with 2x volume DPBS. On-bead digestions were performed for 12 hours at 37 °C with sequence-grade modified trypsin (Promega; 2 µg) in the presence of 2 mM CaCl₂. Peptide samples were acidified to a final concentration of 5% (v/v) formic acid and stored at -80 °C prior to analysis.

LC-MS/MS analysis. Samples were analyzed by multidimensional liquid chromatography tandem mass spectrometry (MudPIT) using an Agilent 1100-series quaternary pump and Thermo Scientific LTQ Orbitrap ion trap mass spectrometer. Peptides were eluted in a 5-step MudPIT experiment using 0%, 25%, 50%, 80%, and 100% salt bumps of 500 mM aqueous ammonium acetate and data were collected in data-dependent acquisition mode with dynamic exclusion turned on (60 s, repeat of 1). Specifically, one full MS (MS1) scan (400-1800 m/z) was followed by 7 MS2 scans of the most abundant ions. The MS2 spectra data were extracted from the raw file using RAW Xtractor (version 1.9.1; publicly available at <http://fields.scripps.edu/downloads.php>). MS2 spectra data were searched using the Sequest algorithm against the latest version of the mouse IPI database concatenated with the reversed database for assessment of false-discovery rates. Sequest searches allowed for static modification of cysteine residues (+57.02146, alkylation), variable methionine oxidation (+15.9949), mass shifts of labeled amino acids (+10.0083 R, +8.0142 K) and no enzyme specificity. The resulting MS2 spectra matches were assembled into protein identifications and filtered using DTASelect (version 2.0) using the --modstat, --mass, and --trypstat options (applies different statistical models for the analysis of methionine oxidation, high resolution masses, and peptide digestion state, respectively). Ratios of light/heavy peaks were calculated using in-house software and normalized at the peptide level to the average ratio of all non-serine hydrolase peptides. Reported ratios represent the mean of all unique, quantified peptides per protein and do not include peptides that were >3 standard deviations from the median peptide value. Proteins with fewer than three peptides per protein ID were not included in the analysis. **Assay Cutoff:** A compound was considered active for a particular target/anti-target with a light/heavy ratio of ≤0.5.

Selectivity analysis by ABPP-SILAC *in situ* (AID 651980)

Assay Overview: The purpose of this assay is to determine the selectivity profile of powder samples of test compounds using stable isotope labeling with amino acids in cell culture (SILAC) ABPP. In this assay, cultured HEK293T cells are metabolically labeled with light or heavy amino acids. Light and heavy cells are treated with inhibitor and DMSO, respectively, *in situ*, followed by the cell-permeable alkyne-functionalized triazole urea ABPP probe NHU5 [12]. NHU5 covalently reacts with a subset of serine hydrolases, including LYPLA2 and LYPLA1, and shows slower reaction kinetics than other cell-permeable serine hydrolase-specific ABPP probes (e.g., FP-alkyne), facilitating analysis of target inhibition by reversible compounds. Cells are harvested, proteome fractions isolated and reacted with a biotin-functionalized azide tag under copper(I)-catalyzed azide-alkyne cycloaddition (“click chemistry”) reaction conditions for enrichment of probe-tagged proteins. Light and heavy samples are combined in a 1:1 (w/w) ratio. Biotinylated proteins are enriched, trypsinized, and analyzed by LC/LC-MS/MS (MudPIT). Inhibition of target and anti-target activity is quantified by comparing intensities of light and heavy peptide peaks. As designed, compounds that act as inhibitors will block NHU5 probe

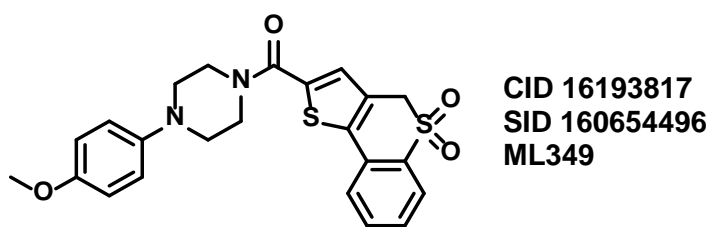
labeling, reducing enrichment in the inhibitor-treated (light) sample relative to the DMSO-treated (heavy) sample, giving a smaller light/heavy ratio for each protein. Proteins not targeted by inhibitors would be expected to have a ratio close to 1.

Sample Preparation. HEK293T cells were initially grown for 6 passages in either light or heavy SILAC DMEM medium supplemented with 10% dialyzed FCS and 1x PenStrep Glutamine in a humidified incubator (37 °C, 5% CO₂). Light medium was supplemented with 100 µg/mL L-arginine (Sigma) and 100 µg/mL L-lysine (Sigma). Heavy medium was supplemented with 100 µg/mL [¹³C₆¹⁵N₄]-L-Arginine (Isotek) and 100 µg/mL [¹³C₆¹⁵N₂]-L-Lysine (Isotek). Light cells were treated with test compound (5 µM) and heavy cells were treated with DMSO for 3 hours at 37 °C. Activity-based alkyne probe NHU5 (50 µM) was added, and cells incubated for 1 hour at 37 °C. After 1 hour, cells were washed (4x DPBS), harvested, isolated by centrifugation at 1,400 x g for 3 minutes, re-suspended in methanol/chloroform/dH₂O (4:1:3 v/v), and vortexed. After centrifugation at 13,000 x g for 3 minutes, the upper layer was removed and 3 volumes of methanol were added and the solution vortexed. Protein was pelleted by centrifugation at 13,000 x g for 6 minutes. The supernatant was removed and the pellet was air-dried and re-suspended in PBS by sonication. Light and heavy proteomes were mixed in 1:1 (w/w) ratio to generate one membrane and one soluble sample. For affinity purification of probe-labeled proteins, click chemistry with a biotin-azide tag (100 µM) was carried out under standard conditions (1 mM TCEP, 100 µM TBTA ligand, 1 mM Cu(II)sulfate, 1 hour, 25 °C), and excess reagents removed by washing the precipitated protein with cold methanol (3 x 750 µL). The protein pellets were resolubilized in 2.5% SDS/DPBS (750 µL) by sonication and heating (60 degrees C, 5 minutes). The concentration of SDS was reduced to 0.5% with DPBS (3 mL), and biotinylated proteins enriched with streptavidin beads (50 µL, 1 hour, 25 °C). The beads were washed with 1% SDS in DPBS (1x), 6 M urea (1x), and DPBS (2x), then resuspended in 6 M urea (150 µL), reduced with 5 mM TCEP for 20 minutes, and alkylated with 10 mM iodoacetamide for 30 minutes at 25 °C in the dark, and the urea concentration was reduced to 2 M with 2x volume DPBS. On-bead digestions were performed for 12 hours at 37 °C with sequence-grade modified trypsin (Promega; 2 µg) in the presence of 2 mM CaCl₂. Peptide samples were acidified to a final concentration of 5% (v/v) formic acid and stored at -80 °C prior to analysis.

LC-MS/MS analysis. Samples were analyzed by multidimensional liquid chromatography tandem mass spectrometry (MudPIT) using an Agilent 1100-series quaternary pump and Thermo Scientific LTQ Orbitrap ion trap mass spectrometer. Peptides were eluted in a 5-step MudPIT experiment using 0%, 25%, 50%, 80%, and 100% salt bumps of 500 mM aqueous ammonium acetate and data were collected in data-dependent acquisition mode with dynamic exclusion turned on (60 s, repeat of 1). Specifically, one full MS (MS1) scan (400-1800 m/z) was followed by 7 MS2 scans of the most abundant ions. The MS2 spectra data were extracted from the raw file using RAW Xtractor (version 1.9.1; publicly available at <http://fields.scripps.edu/downloads.php>). MS2 spectra data were searched using the Sequest algorithm against the latest version of the mouse IPI database concatenated with the reversed database for assessment of false-discovery rates. Sequest searches allowed for static modification of cysteine residues (+57.02146 due to alkylation), variable methionine oxidation (+15.9949), mass shifts of labeled amino acids (+10.0083 R, +8.0142 K) and no enzyme

specificity. The resulting MS2 spectra matches were assembled into protein identifications and filtered using DTASelect (version 2.0) using the --modstat, --mass, and --trypstat options (applies different statistical models for the analysis of methionine oxidation state, high resolution masses, and peptide digestion state, respectively). Ratios of light/heavy peaks were calculated using in-house software and normalized at the peptide level to the average ratio of all non-serine hydrolase peptides. Reported ratios represent the mean of all unique, quantified peptides per protein and do not include peptides that were >3 standard deviations from the median peptide value. Proteins with fewer than three peptides per protein ID were not included in the analysis. **Assay Cutoff** A compound was considered active for a particular target/anti-target with a light/heavy ratio of ≤ 0.5 .

2.2 Probe Chemical Characterization

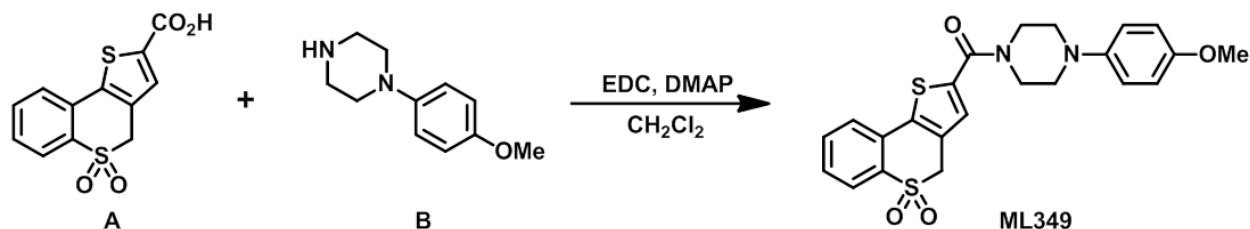


The probe structure was verified by ^1H and ^{13}C NMR (see **Section 2.3**) and high resolution MS (m/z calculated for $\text{C}_{23}\text{H}_{22}\text{N}_2\text{O}_4\text{S}^2$ $[\text{M}+\text{H}]^+$: 455.1094; found, 455.1095. Purity was assessed to be greater than 95% by NMR. Solubility (room temperature) was determined to be $<1\ \mu\text{M}$ in PBS, $0.5\ \mu\text{M}$ in DMEM, and $8.6\ \mu\text{M}$ in DMEM containing 10% fetal calf serum. The latter buffer conditions are more relevant to biological experiments (complex proteome, cell-based studies in serum-containing medium, *in vivo*), and we have not found the solubility to be a hindrance for biological application (**Sections 3.5** and **3.6** and ref. [12]). However, gel-based ABPP anti-target selectivity data collected at $10\ \mu\text{M}$ compound concentration (**Sections 3.4** and **3.6**) should be treated with some caution given the lower solubility limits; however, all cell-based potency (**Section 3.5**) and SILAC-ABPP selectivity studies (**Section 3.6**) were conducted with compound concentrations below solubility limits. Stability in PBS was determined to be >48 hours.

Table 2.2-1. Compounds submitted to the SMR collection.

Designation	CID	SID	SRID	MLS
Probe	16193817	160654496	SR-01000775306-4	MLS004819995
Analog 1	70697699	160709337	SR-02000002491-1	MLS004819996
Analog 2	70697697	160709338	SR-02000002492-1	MLS004819997
Analog 3	70697706	160709343	SR-02000002497-1	MLS004819998
Analog 4	70697709	160709344	SR-02000002498-1	MLS004819999
Analog 5	70697700	160709345	SR-02000002499-1	MLS004820000
Analog 6	11957183	161004944	SR-01000687879-3	MLS004820344
Analog 7	1316101	161004948	SR-01000679418-4	MLS004820345
Analog 8	23602465	161004943	SR-02000002342-2	MLS004820346
Analog 9	23602694	161004942	SR-02000002345-2	MLS004820347

2.3 Probe Preparation



(5,5-Dioxido-4H-thieno[3,2-c]thiochromen-2-yl)(4-(4-methoxyphenyl)piperazin-1-yl)methanone (ML349)

To a solution of 4H-thieno[3,2-c]thiochromene-2-carboxylic acid 5,5-dioxide (**A**, 25 mg, 0.089 mmol) in dichloromethane (1.0 mL) were added 1-(4-methoxyphenyl)piperazine (**B**, 17 mg, 0.089 mmol), EDC (51 mg, 0.267 mmol) and 4-DMAP (catalyst) at room temperature. After stirring for 12 hours at room temperature, the reaction was quenched with 3.0 mL of saturated aqueous NaHCO₃ solution. The organic layer was separated and the aqueous layer was extracted with dichloromethane. The combined organic extracts were washed with brine, dried over MgSO₄, filtered and concentrated. The crude product was purified by flash column chromatography using a 97:3 v/v dichloromethane:methanol as solvent to afford the desired compound (35 mg, 87 % yield) as a yellow solid. ¹H NMR 400 MHz (CDCl₃): δ 8.05 - 8.03 (*d*, *J* = 7.6 Hz, 1H), 7.68 - 7.61 (*m*, 2H), 7.56 - 7.52 (*t*, *J* = 7.6 Hz, 1H), 7.21 (*s*, 1H), 6.93 - 6.91 (*m*, 2H), 6.87 - 6.85 (*m*, 2H), 4.44 (*s*, 2H), 3.93 (*m*, 4H), 3.78 (*s*, 3H), 3.13 (*m*, 4H); purity > 95%. ¹³C NMR 133 MHz (CDCl₃): δ 162.5, 154.9, 145.4, 137.7, 136.6, 134.3, 133.9, 130.4, 130.2, 129.6, 128.2, 126.2, 124.6, 119.4, 114.9, 77.6, 77.1, 55.9, 51.6. HRMS (*m/z*): [M+H]⁺ calculated for C₂₃H₂₂N₂O₄S₂: 455.1094; found, 455.1095.

3 Results

As determined by gel-based ABPP, probe ML349 has an IC₅₀ value of 144 nM *in vitro* against LYPLA2 (**Section 3.2**). Out of more than 20 SHs (including lipases, esterases, proteases, and uncharacterized hydrolases) profiled by gel-based ABPP, ML349 is observed to have no off-targets (up to 10 μM, **Sections 3.4** and **3.6**), including close homolog LYPLA1 (up to 3 μM, **Section 3.2**), affording a good selectivity window for target inhibition. ML349 does not exhibit overt cytotoxicity, has sufficient solubility in serum-containing medium (8.6 μM) for biological characterization (**Sections 3.5** and **3.6**), shows good chemical stability (>48 hours), and no overt chemical reactivity (**Section 2.2**). Importantly, ML349 target engagement has been demonstrated both *in situ* and *in vivo* (**Section 3.5**). Selectivity for the probe was also confirmed by in-depth LC-MS/MS profiling of 30+ other SHs *in vitro* and *in situ* by ABPP-SILAC as detailed in **Section 3.6**.

3.1 Summary of Screening Results

In the primary fluopol-ABPP HTS [17] assay for LYPLA2 (AID 2177), ~315K compounds were screened with the SH-specific FP-Rh probe [15]. A total of 1197 compounds (0.38%) were active, passing the set threshold of 25.78% LYPLA2 inhibition. For the confirmation HTS screen (AID 2232), 1098 active compounds were retested in triplicate, and 790 compounds (72%) were confirmed as active (**Figure 3.1-1**).

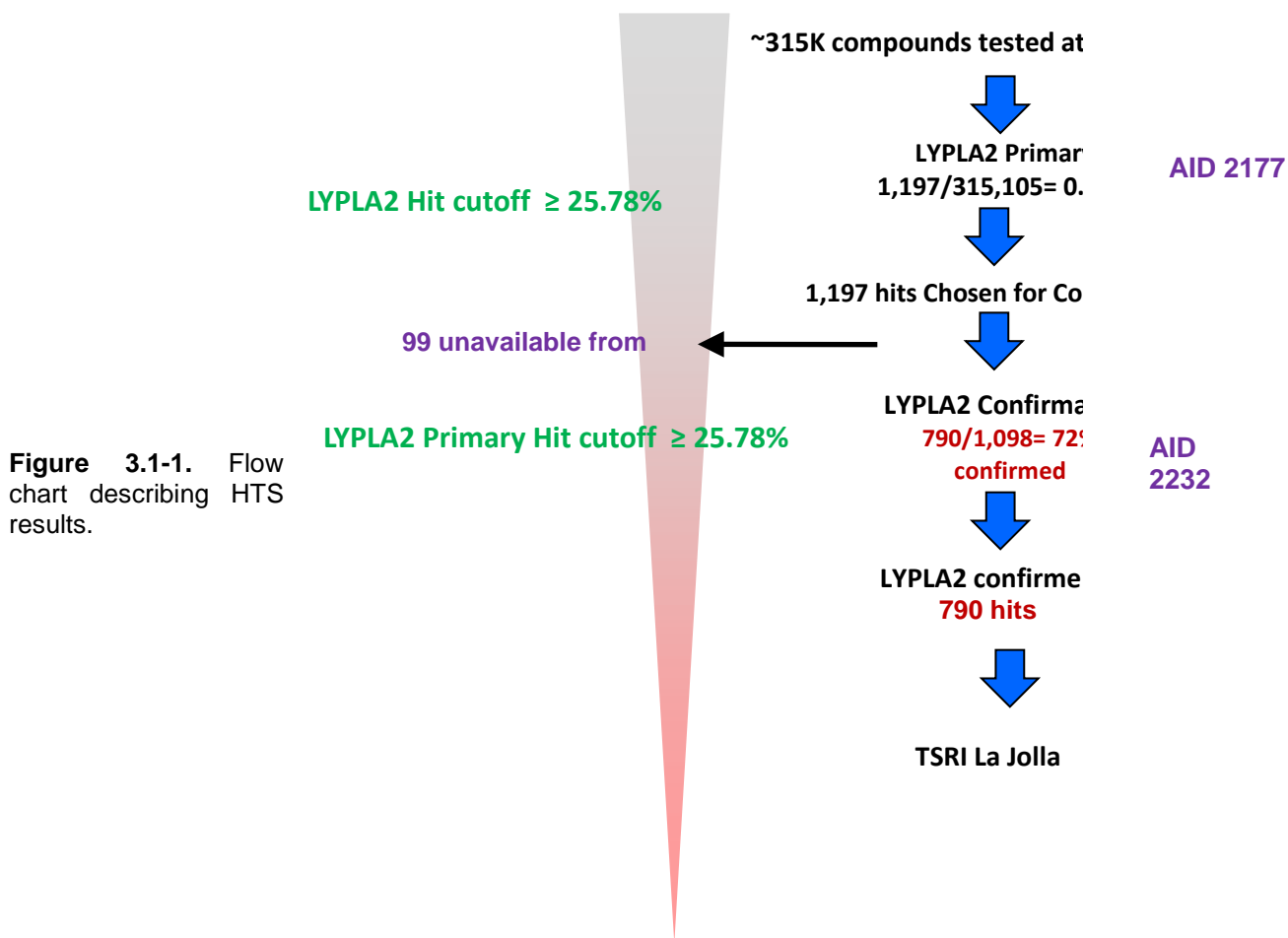


Figure 3.1-1. Flow chart describing HTS results.

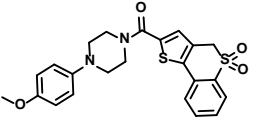
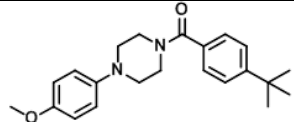
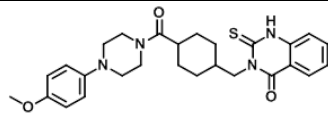
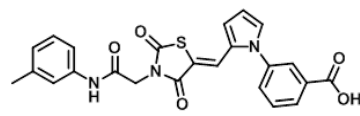
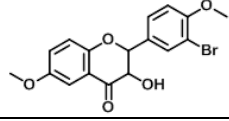
Prior to secondary screening, the active compounds were filtered to remove compounds with at least 30% activity against previous fluopol-ABPP enzyme inhibitor screens: GSTO1 (AID 1974; 36 compounds), PME-1 (AID 2130, 8 compounds), and LYPLA1 (AID 2174; 50 compounds). Additionally, 14 compounds with greater than 5% hit rate in all bioassays tested were removed. Of the remaining compounds, all available hits with at least 50% inhibition against LYPLA2 (154 compounds) were subject to gel-based ABPP secondary screening. (Note: dual LYPLA1/LYPLA2 hit compounds not tested here were assayed as described in the Probe Report for ML211).

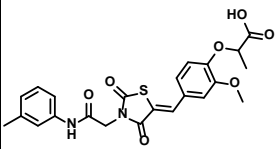
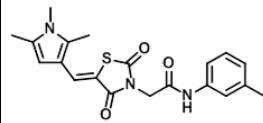
The 154 compounds were assayed for their ability to inhibit recombinant human (rh) LYPLA2 by gel-based competitive ABPP [12, 16] in the context of a complex proteome (AID 652029;

Supplemental **Figures S1** and **S2** and **Table S1**). ABPP is a highly established platform for enzyme activity profiling and inhibitor development, and the methodology is in ubiquitous use by the biological community (e.g., see reviews [18-21]). By nature, activity-based probes (e.g., the SH-specific fluorophosphonate [FP] probes) are active-site directed, reporting directly on the activity state of the enzyme. As such they give the same type of readout as a substrate-based assay (as previously demonstrated for other SHs, e.g., FAAH [16], KIAA1363 [22], and MAGL [23]), providing crucial details regarding probe concentration and treatment time needed to inactivate the enzyme. Moreover, ABPP assays are readily applied for assessing enzyme activity both *in situ* (live cells) and *in vivo* (animal models), **Sections 3.5** and **3.6** [12].

In this gel-based assay, a complex mouse brain proteome (chosen for its number and diversity of gel-resolvable SHs for optimal selectivity profiling) containing endogenous and spiked-in recombinant forms of LYPLA2, is incubated with test compound (20 μ M) followed by reaction with the fluorescently-tagged activity-based probe fluorophosphonate-rhodamine (FP-Rh). The reaction products are separated by SDS-PAGE and visualized in-gel using a flatbed fluorescence scanner. Test compounds that act as LYPLA2 inhibitors will prevent enzyme-probe interactions, thereby decreasing the fluorescence intensity of the protein bands. Of the 154 compounds tested, 39 exhibited at least 50% inhibition of LYPLA2 (AID 652029). The top hits from this assay, as well as 10 compounds that registered as LYPLA2-selective from AID 493105 (secondary gel-based ABPP screening for LYPLA1-selective and dual LYPLA1/LYPLA2 inhibitors) were rescreened against rhLYPLA2 and endogenous mouse (em) LYPLA2 and emLYPLA1 at a lower (10 μ M) compound concentration. Seven compounds (**Table 3.1-1**) showed good inhibition (>30%) for both rhLYPLA2 and emLYPLA2 and reduced activity (<30%) for anti-target emLYPLA1.

Table 3.1-1. Top LYPLA2-selective inhibitors from gel-based 2ary Screen (see supplemental for complete results)

Cpd # (Figures S1 and S2)	SID	CID	Structure	% Inhibition (10 μ M test cpd)		
				rhLYPLA2	emLYPLA2	emLYPLA1
ML349	92709328	16193817		79%	74%	25%
166 (cpd 7 in Table 3.4- 1)	92709285	1316101		57%	47%	16%
61	4245654	3240101		47%	44%	16%
173	92709303	11839276		66%	77%	17%
58	14728505	6917582		47%	55%	23%

124	92709371	6520605		58%	37%	28%
150	92709291	2252839		51%	40%	9%

The top lead (CID 16193817, subsequently designated ML349), as well as compounds **166** and **61** possess a piperazine amide core with a 4-methoxyphenyl substituent, which was the initial focus of the SAR campaign as detailed in **Section 3.4**.

3.2 Dose Response Curves for Probe

In vitro IC₅₀ values for ML349 against target LYPLA2 (IC₅₀ of 144 nM) and anti-target LYPLA1 (IC₅₀ > 3000 nM) were obtained from gel-based competitive-ABPP data using the FP-PEG-Rh activity-based probe in a complex proteome lysate against the endogenous human enzyme (AID 651990) [12] (**Figure 3.2-1**). FP-PEG-Rh was utilized for this study as it exhibits slower labeling kinetics than the more widely utilized ABPP probe FP-Rh, facilitating analysis of reversible inhibitors like ML349 (see **Section 3.3** and ref. 12).

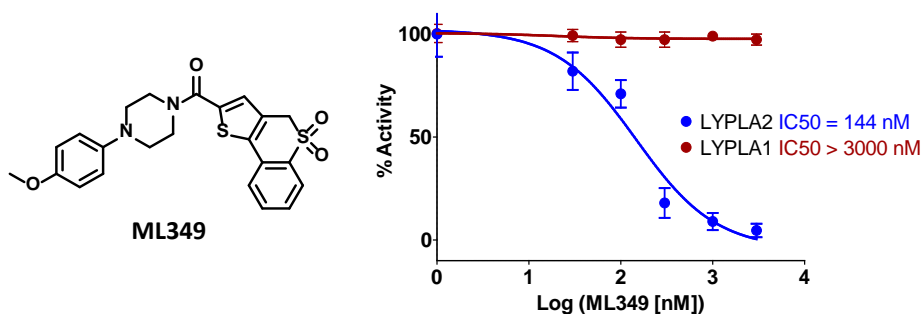


Figure 3.2-1. IC₅₀ curves for probe ML349 (SID 160654496) for target LYPLA2 and anti-target LYPLA1 as determined by gel-based competitive-ABPP with the activity-based probe FP-PEG-Rh against endogenous human enzyme in a complex proteome (HEK293T soluble proteome). Data are presented as means \pm s.e.m. for 3 independent experiments. (AID 651990).

In a complementary substrate assay with purified, recombinant human enzyme, an IC₅₀ of 510 nM and K_i of 230 nM were calculated for ML349 inhibition of LYPLA2 (**Figure 3.2-2**). Given the different experimental conditions (endogenous vs. purified enzyme), some difference in calculated IC₅₀s vs. gel-based ABPP (**Figure 3.2-1**) is to be expected. Little (<50%) inhibition of anti-target LYPLA1 was observed up to ~10 μ M under the same conditions.

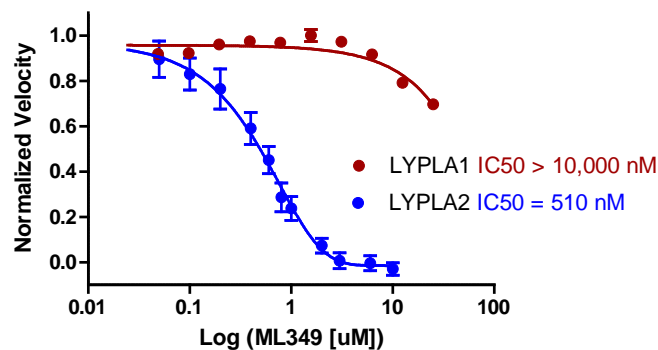
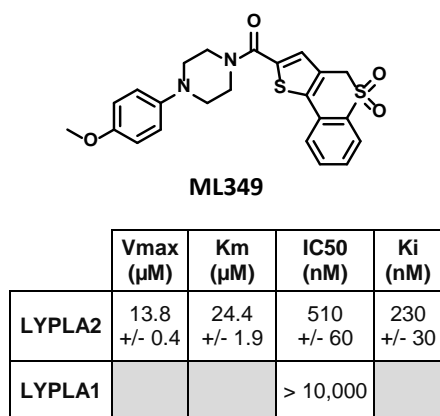


Figure 3.2-2. IC₅₀ curves for probe ML349 (SID 160654496) for target LYPLA2 and anti-target LYPLA1 as determined by fluorogenic resorufin acetate substrate hydrolysis assay with 10 nM purified recombinant human LYPLA2 and LYPLA1; graph shows inhibition of substrate turnover upon treatment with ML349 (AIDs 652001 and 652003). V_{max} and K_m values were derived from Michaelis-Menten kinetic analysis (AIDs 652001); K_i value was derived using the Cheng-Prusoff equation (AID 652001). Data are presented as means +/- s.e.m. for 4 independent experiments.

3.3 Scaffold/Moiety Chemical Liabilities

ML349 lacked any obvious electrophilic moieties for covalent enzyme modification, suggesting that the probe operated by a reversible mechanism. This hypothesis was confirmed by gel filtration studies, which demonstrated near-complete recovery of ABPP probe (FP-PEG-Rh) labeling for LYPLA2 after two rounds of gel filtration to remove small molecules (e.g., inhibitor compounds) as shown in **Figure 3.3-1** (AID 651987) [12]. For comparison, even three rounds of gel filtration did not result in recovery of ABPP probe labeling when LYPLA1 and LYPLA2 were treated with the covalent triazole urea inhibitor **AA26-9**. Prior LC-MS/MS characterization has determined that compounds of the triazole urea class like **AA26-9** inactivate their SH targets by irreversible carbamoylation of the catalytic serine [24]. Likewise, ML349 did not show any reactivity with glutathione (50 μM , 6 hrs).

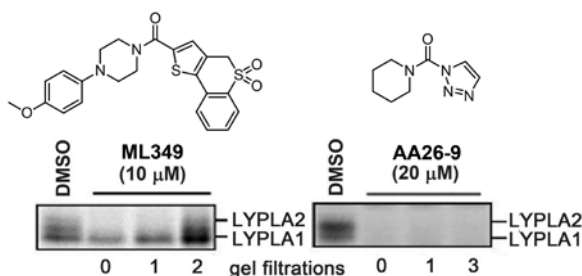


Figure 3.3-1. Gel Filtration studies reveal that ML349 is a reversible inhibitor (left); treatment with irreversible inhibitor **AA26-9** shown for comparison (right). Soluble HEK293T proteome was treated with test compound or DMSO (control) for 30 minutes. Aliquots were removed from each sample, and the remaining sample passaged over a gel filtration column. Samples were reacted with FP-PEG-Rh and analyzed by SDS-PAGE. Fluorescent images shown in grey scale. (AID 651987).

3.4 SAR Tables

The SAR **Tables 3.4-1** and **3.4-2** include 24 purchased and synthetic compounds: the initial top two hits from HTS (ML349 and cpd **7** in **Table 3.4-1**; note: cpd **7** also listed as cpd **66** in **Table 3.1-1** and supplemental), 11 other reversible analogs (**Table 3.4-1**) and 14 analogs based on a triazole urea scaffold (**Table 3.4-2**). We previously identified a triazole urea (SID 7974398) as a top lead in the HTS assay for LYPLA1 inhibitors (AID 2174), and have subsequently derived triazole urea probes for LYPLA1/LYPLA2 (ML211), PAFAH2 (ML225), ABHD11 (ML226), DAGL β (ML294), and ABHD6 (ML295) as shown in **Figure 3.4-1**. As a class, the triazole ureas were found to have tunable potency and selectivity, low cytotoxicity, and good activity *in situ* and *in vivo* (see respective Probe Reports and refs. [24, 25]). As such, we thought it might be possible to graft structural elements of the successful reversible LYPLA2 inhibitors onto the triazole urea core; however, as discussed below, selectivity vs. LYPLA1 was not preserved with this series of analogs.

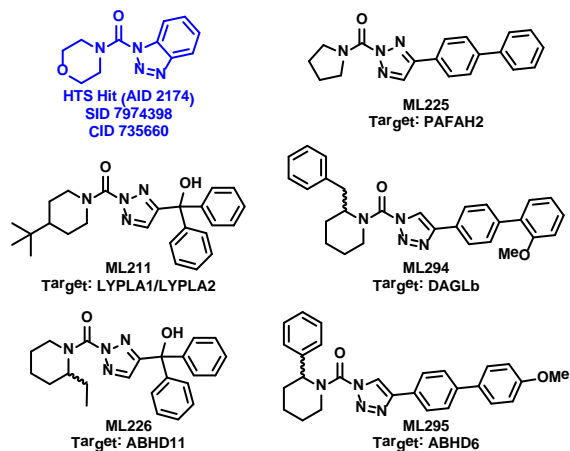


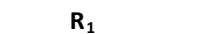

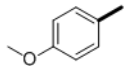
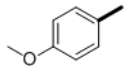
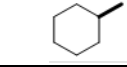
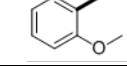
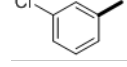
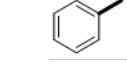
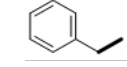

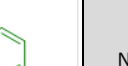
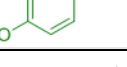
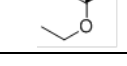

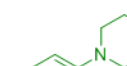
Figure 3.4-1. Structures of triazole urea HTS hit and derived SH Probes.

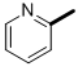
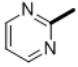
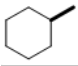
As summarized in the tables below, SAR compounds were subject to gel-based competitive ABPP profiling [12, 16] to assess potency and selectivity against several dozen FP-sensitive SHs in the HEK293T proteome, which endogenously expresses target LYPLA2 and anti-target LYPLA1 (**Figure 3.6-1**). For this assay, we modified the ABPP conditions previously employed for HTS hit evaluation (**Section 3.1** and supplemental) to optimize for assessment of reversible inhibitors by utilizing an FP-PEG-Rh probe, which has slower labeling kinetics than the standard FP-Rh serine-hydrolase specific ABPP probe, minimizing out-competition [12]. Compounds were tested at 300 nM, 1 μ M, and 10 μ M concentration.

As noted in **Section 2.2**, the solubility determined for ML349 (8.6 μ M) is somewhat below the 10 μ M test compound concentration. As such, some of the anti-target data collected at 10 μ M should be treated with caution; however, even if anti-target selectivity is calculated using 8.6 μ M as an upper limit, selectivity is still more than sufficient for complete inactivation of LYPLA2 without apparent anti-target effects.

To investigate the SAR around the piperazine amide core of ML349, compounds **2-13** were obtained from commercial vendors and evaluated by gel-based competitive ABPP (see **Table 3.4-1** for summary and **Section 3.6** for gel images). Overall, the SAR profile was rather steep, with only analogs **7**, **9**, and **10** showing good inhibition at 1 μM test compound concentration. ML349 and these three select analogs are distinguished by 4-substituted phenyl groups at **R₁** (e.g., vs. **3**, **4**, and **5**), suggesting this structural element is key to activity. However, none of the analogs exhibited potency rivaling that of ML349. In terms of selectivity, none of the compounds in the piperazine amide series showed evidence of significant inhibition of other SH anti-targets by gel-based profiling, even at the highest test concentration (10 μM). As noted above in **Section 2.2**, this value is slightly outside the range of solubility for ML349, so these results should be treated with some caution; however, setting an upper limit of 8.6 μM still provides a large (60-fold) selectivity window for inhibition of LYPLA2 (IC₅₀ of 144 nM, **Section 3.2**) vs. all other SHs profiled by gel-based ABPP. It is of note that the identified probe ML348 (**Figure 1-1**, see ML348 Probe Report) for anti-target LYPLA1, which shares high (65%) sequence identity with LYPLA2, also exhibits a piperazine amide core, suggesting that the scaffold is a privileged chemotype for selective inhibition of this subfamily of SHs.

Table 3.4-1. Piperazine Amide SAR

Compound lab name	SID †	CID	SRID	Structure **		IC50 (nM) (AID 651990) §		% Inhibition (AID 651988) ¥						fold selectivity LYPLA2 vs. LYPLA1 (AID 651988)
						LYPLA2	LYPLA1	LYPLA2			LYPLA1			
								0.3 μM	1 μM	10 μM	0.3 μM	1 μM	10 μM	
1 (ML349)	160654495 (commercial)	16193817	SR-01000775306-3		H	ND ‡	ND	100	100	100	0	0	0	>33
	160654496 (resynthesized)		SR-01000775306-4		H	144	>3000	ND	ND	ND	ND	ND	ND	>21*
2	160654505	22334665	SR-02000002338-1		H	ND	ND	0	0	25	0	0	0	ND
3	160654506	23602396	SR-02000002339-1		H	ND	ND	0	0	0	0	0	0	ND
4	160654507	23602401	SR-02000002340-1		H	ND	ND	0	0	0	0	0	0	ND
5	160654508	23602403	SR-02000002341-1		H	ND	ND	0	25	75	0	0	0	>1
6	160654492	11957183	SR-01000687879-2		H	ND	ND	0	0	50	0	0	0	>1
7	160654491	1316101	SR-01000679418-3			ND	ND	0	75	75	0	0	0	>10
8	160654494	16193813	SR-01000746406-2		Cl	ND	ND	0	0	0	0	0	0	ND
9	160654500	8294576	SR-01000859016-3			ND	ND	25	100	100	0	0	0	>10
10	160654509	23602465	SR-02000002342-1		H	ND	ND	25	100	100	0	0	0	>10

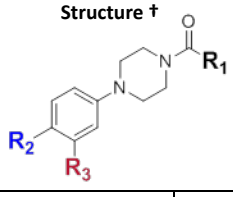
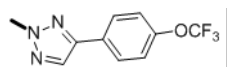
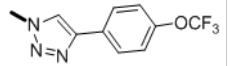
11	160654510	23602645	SR-02000002343-1		Cl	ND	ND	0	0	0	0	0	0	ND
12	160654511	23602666	SR-02000002344-1		Cl	ND	ND	0	25	75	0	0	0	>1
13	160654512	23602694	SR-02000002345-1		Cl	ND	ND	25	25	75	0	0	0	>1

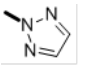
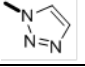
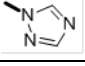
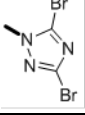
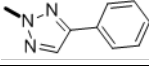
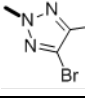
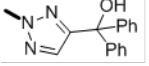
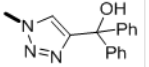
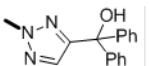
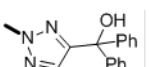
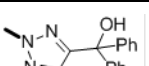
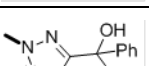
† All compounds were purchased with the exception of 160654496 (ML349), which was synthesized
 ** R1/R2 not applicable to structures shown in green (7 and 9)
 § IC50 values were determined from three replicates at each inhibitor concentration
 ¥ % Inhibition values were determined from one replicate at each inhibitor concentration
 ‡ ND = not determined
 * calculated as >3,000 nM / 144 nM (highest test conc. at which less than 50% inhibition was observed for LYPLA1 divided by IC50 for LYPLA2)

As mentioned above, we previously optimized a dual LYPLA1/LYPLA2 inhibitor (**ML211**, **Figure 1.1** and **Figure 3.4-1**) based on the triazole urea scaffold as identified in an HTS hit compound (**Figure 3.4-1**). We hoped to combine structural elements of the reversible compound **ML349** with the core triazole urea scaffold to derive a selective LYPLA2 inhibitor. As such, we preserved the left hand piperazine amide of **ML349** bearing the 4-methoxyphenyl substituent at **R₁** and replaced the fused cyclic system with a series of 2,4- and 1,4-triazoles (**Table 3.4-2**). These compounds all had some inhibitory activity for LYPLA2 and LYPLA1; however, none exhibited sufficient LYPLA2 vs. LYPLA1 selectivity to merit further pursuit.

Finally, we resynthesized ML349 as SID 160654496 (**Table 3.4-1**) as described in **Section 2.3** and confirmed structure by 1H-NMR and HRMS as detailed in **Section 2.2**. Inhibitory activity for LYPLA2 and selectivity vs. LYPLA1 was confirmed by competitive ABPP (IC50 = 144 nM for LYPLA2, > 3000 nM for LYPLA1, **Section 3.2**).

Table 3.4-2. Triazole Urea SAR

Compound lab name	SID	CID	SRID	Structure †			% Inhibition (AID 652018) ¥						fold selectivity LYPLA2 vs. LYPLA1 (AID 652018)	# of Other Anti-targets (AID 652018)		
					R ₂	R ₃	LYPLA2			LYPLA1				0.3 μM	1 μM	10 μM
							0.3 μM	1 μM	10 μM	0.3 μM	1 μM	10 μM				
JW817	160709336	70697711	SR-02000002490-1		OMe	H	10	10	20	10	10	20	ND ‡	0	0	0
JW817(1,4)	160709347	70697688	SR-02000002501-1		OMe	H	10	10	60	20	20	80	0	0	0	0

JW823	160709337	70697699	SR-0200000 2491-1		OMe	H	10	60	100	20	80	95	0	0	0	0
JW823(1,4)	160709348	70697689	SR-0200000 2502-1		OMe	H	10	30	85	20	50	90	0	0	0	0
JW824	160709338	70697697	SR-0200000 2492-1		OMe	H	10	30	95	20	75	95	0	0	0	0
JW825	160709339	70697703	SR-0200000 2493-1		OMe	H	10	30	95	20	60	95	0	0	0	0
JW826	160709340	70697693	SR-0200000 2494-1		OMe	H	10	30	30	20	30	30	ND	0	0	0
JW827	160709341	70697705	SR-0200000 2495-1		OMe	H	50	80	100	85	95	95	0	0	0	2
JW829	160709342	70697695	SR-0200000 2496-1		OMe	H	75	100	100	95	95	95	0	0	0	1
JW829(1,4)	160709349	70697691	SR-0200000 2503-1		OMe	H	20	95	100	85	95	95	0	0	0	2
JW880	160709343	70697706	SR-0200000 2497-1		Cl	Cl	20	30	30	30	40	80	ND	0	0	0
JW881	160709344	70697709	SR-0200000 2498-1		Br	H	20	30	80	40	90	100	ND	0	0	0
JW882	160709345	70697700	SR-0200000 2499-1		CF ₃	H	20	30	30	30	30	30	ND	0	0	0
JW883	160709346	70697692	SR-0200000 2500-1		H	CF ₃	20	30	30	25	30	30	ND	0	0	0

† All compounds are synthetic compounds
‡ % Inhibition values were determined from one replicate at each inhibitor concentration
‡ ND = not determined

3.5 Cellular Activity

In situ Inhibition: LYPLA2 probe ML349 (SID 160654496) and LYPLA1 Probe ML348 (SID 160654487; see **Figure 1-1** or **3.4-1** for structure and ML348 Probe Report for more details) are active *in situ* against both the human and mouse isoforms of LYPLA enzymes (AID 651986) as assessed by gel-based competitive ABPP following three hours of compound treatment (5 μ M) and *in situ* competition with cell-permeable alkyne ABPP probe NHU5 (see **Figure 3.6-4** for structure [25]). NHU5 labels a subset of SHs with slower kinetics than other SH-selective alkyne probes (e.g., FP-alkyne [12]), thus facilitating competitive ABPP under kinetically controlled conditions. NHU5 can be affixed with a rhodamine-azide (Rh-azide) reporter tag following cell lysis using the Cu(I)-catalyzed azide-alkyne cycloaddition 'click chemistry' reaction for fluorescent visualization following SDS-PAGE. As shown in **Figure 3.5-1**, both probes selectively inhibit their respective targets in cultured cells, and direct, *in situ* competition with a membrane-permeable click ABPP probe allows for direct readout of target engagement [12]. A more in-depth LC-MS/MS-based ABPP-SILAC analysis of *in situ* selectivity of ML349 is detailed in **Section 3.6**.

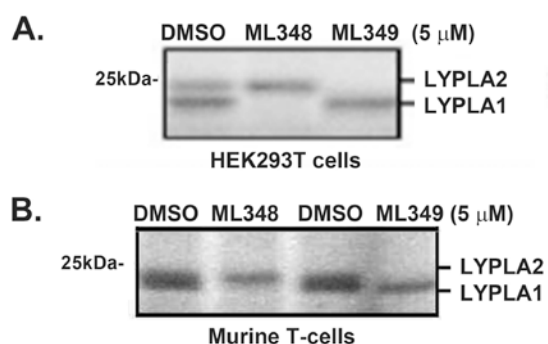


Figure 3.5-1. *In situ* inhibition of LYPLA2 and anti-target LYPLA1 by ML349 (SID 160654496) and ML348 (SID 160654487), respectively. HEK293T cells (**A**) or murine T-cells (**B**) cultured in medium supplemented with 10% FCS were treated with compound (5 μ M) or DMSO for 3 hours followed by the cell-permeable alkyne-functionalized ABPP probe NHU5 (50 μ M). Cells were washed, harvested, and lysed, and NHU5-labeled proteins conjugated with a Rh-azide reporter tag by click chemistry for fluorescent visualization by gel-based competitive ABPP. ML349 and ML348 show potent inhibition of their respective targets. Fluorescent images shown in grey scale. (AID 651986).

In vivo Inhibition: We also assessed the *in vivo* inhibitory activity of probes ML349 (SID 160654496) and ML348 (SID 160654487) as detailed in AID 651985 and ref. [12]). For this experiment, mice were administered test compound (50 mg/kg, i.p.) or vehicle only. In analogous fashion to the *in situ* competitive ABPP experiment described above, after three hours, mice were then administered NHU5 probe (100 mg/kg, i.p.). After one hour mice were sacrificed and their tissues (brain, heart, kidney, lung, and liver) removed, homogenized, and NHU5-probe labeled proteins conjugated with the Rh-azide reporter tag by click chemistry for fluorescent visualization following SDS-PAGE (**Figure 3.5-2**). Complete or near-complete inhibition of their respective targets (LYPLA2 for ML349, LYPLA1 for ML348) is observed in heart, kidney, and lung. In contrast, only ~50% inhibition is observed in the brain, suggesting limited CNS penetration for this compound class. No inhibition is observed in liver, where the compounds are likely rapidly metabolized. Among the 20+ distinct SH bands, no significant anti-target inhibition is observed in any tissue; these clean profiles indicate that both probes are active and selective *in vivo*, and reveal tissue-restricted target inhibition.

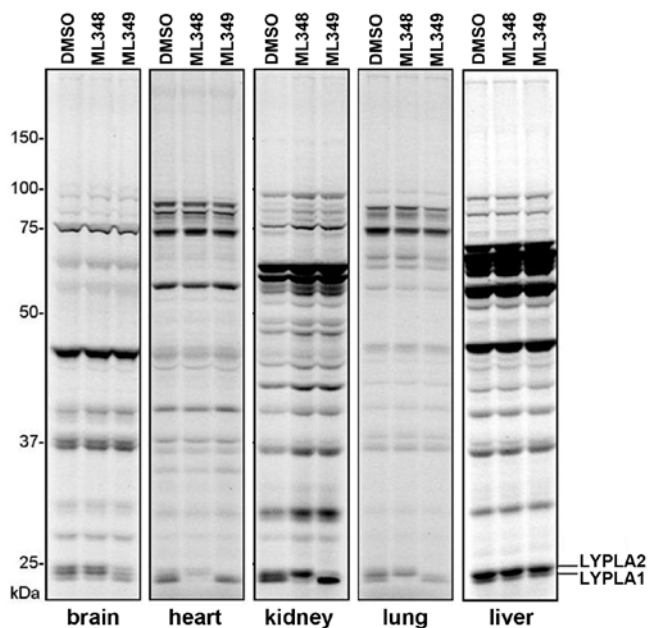


Figure 3.5-2. Both ML349 (SID 160654496) and ML348 (SID 160654487) show potent and selective activity *in vivo*. Mice were administered test compound (50 mg/kg, i.p., 3 hours) or vehicle only followed by the NHU5 alkyne SH ABPP probe (100 mg/kg, i.p.). After 1 hour, mice were sacrificed and tissues removed, homogenized, and clicked with Rh-azide for fluorescent detection following SDS-PAGE. Complete/near-complete inhibition of their respective target enzymes (LYPLA2 for ML349 and LYPLA1 for ML348) is observed in heart, kidney and lung. In contrast, no inhibition is observed in liver and only ~50% inhibition is observed in brain. No other anti-targets are observed among the 20+ distinct bands, indicating clean selectivity *in vivo*. Fluorescent images shown in grey scale. (AID 651985).

Cytotoxicity: The probe ML349 (SID 160654496) and compound **10** (SID 160654509) were evaluated for cytotoxicity (AID 651991) in HEK293T cells cultured in both serum-free and serum-supplemented medium. As shown in **Figure 3.5-3**, the compounds did not show evidence of cytotoxicity under either condition up to 50 μ M test concentration. It should be noted, however, that the solubility of ML349 was determined to be 0.5 μ M in DMEM medium alone and 8.6 μ M in DMEM medium containing 10% serum. As such, the results of the experiments should be interpreted with caution. However, if 8.6 μ M is used as an upper limit on cytotoxicity (in the more biologically-relevant serum-supplemented conditions), that value is still above the *in situ* dosing for complete target inhibition (5 μ M, **Figure 3.5-1**), giving an adequate window for use in cell-based assays.

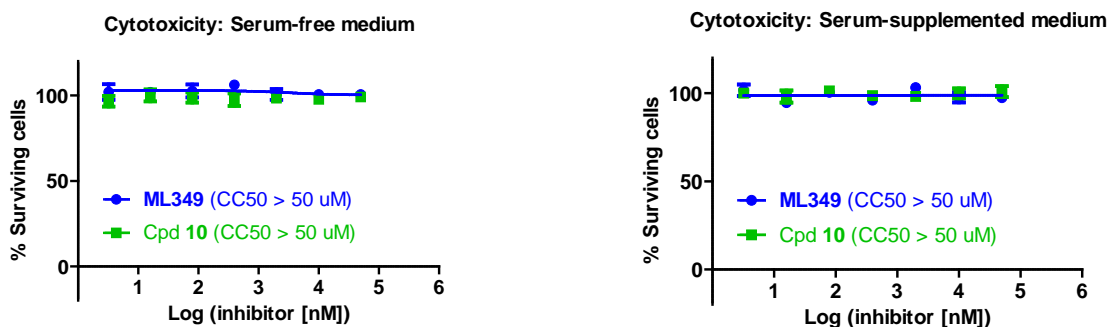


Figure 3.5-3. Cytotoxicity analysis of probe ML349 (SID 160654496) and compound **10** (SID 160654509) in serum-free (**left**) and serum-supplemented (**right**) medium. HEK293T cells cultured in DMEM medium with and without 10% FCS were treated with test compound and viability was assessed using the WST-1 assay (Roche) after 48 hours. CC50 values should be interpreted with caution given the probe's lower solubility (0.5 μ M in serum-free medium and 8.6 μ M in serum-supplemented medium); however, it appears that neither compound show any evidence of overt toxicity at doses above those needed to achieve complete target inhibition *in situ* (5 μ M, **Figure 3.5-1**). (AID 651991).

3.6 Profiling Assays

HTS Assays: To date, ML349 (CID 16193817) has been tested in 500 other high-throughput cell-based and non-cell based bioassays deposited in PubChem, and has shown activity in only 7 of those assays, giving a hit rate of 1.4%. Among target-specific assays, the compound registered modest, unconfirmed activity at relatively high – 3 to 50 μM – test concentrations for: NPY receptors [AIDs 1304 and 1359], MEK kinase [AID 1531], TAAR1 [AID 624466], and GNA15 [AID 651780]. This low hit rate suggests that this compound is not generally active; however, investigation of these possible inhibitor-target interactions could be the subject of future investigation.

Gel-based Competitive ABPP: This medium-throughput proteome-wide screening technique is an invaluable method for characterizing both reversible and irreversible inhibitors (**Section 3.4**), allowing rapid assessment of potency and selectivity among SHs (including lipases, esterases, proteases, and uncharacterized hydrolases), as visualized by disappearance of bands in compound-treated lanes relative to the DMSO-only control. It should be noted that gel-based profiling gives access to fairly low abundant proteins. For example, we have previously determined that we could detect the SH fatty acid amide hydrolase (FAAH) at concentrations as low as 0.0005% of the total proteome (~200 copies per cell) by gel-based ABPP [15].

Probe ML349 (SID 160654496) and analogs listed in **Tables 3.4-1** and **3.4-2** have been subject to gel-based competitive ABPP screening to assess SH reactivity against more than 20 FP-sensitive SHs visible by 1D SDS-PAGE separation and fluorescent detection in the HEK293T proteome (**Figures 3.6-1** and **3.6-2**, AIDs 651988 and 652018). Compound treatment (300 nM, 1 μM , or 10 μM , 30 minutes) was followed by labeling with FP-PEG-Rh (5 μM , 30 minutes), SDS-PAGE, and in-gel fluorescent visualization of FP-labeled proteins. Assignment of LYPLA1/2 bands was based on correlation of molecular weights, expression and inhibition profiles with LC-MS/MS data [24,26] and recombinant enzyme expression [26]. Proteins are listed as anti-targets (**Section 3.4**) if at least 50% inhibition is observed as quantified relative to the DMSO control. Probe solubility may be slightly compromised at the highest (10 μM) concentration, as ML349 would be expected to have solubility in a complex proteome lysate similar to that for FCS-containing medium (8.6 μM). No significant anti-target activity is observed for ML349 at any test concentration, whereas some of the other analogs show potent inhibition of close homolog LYPLA2.

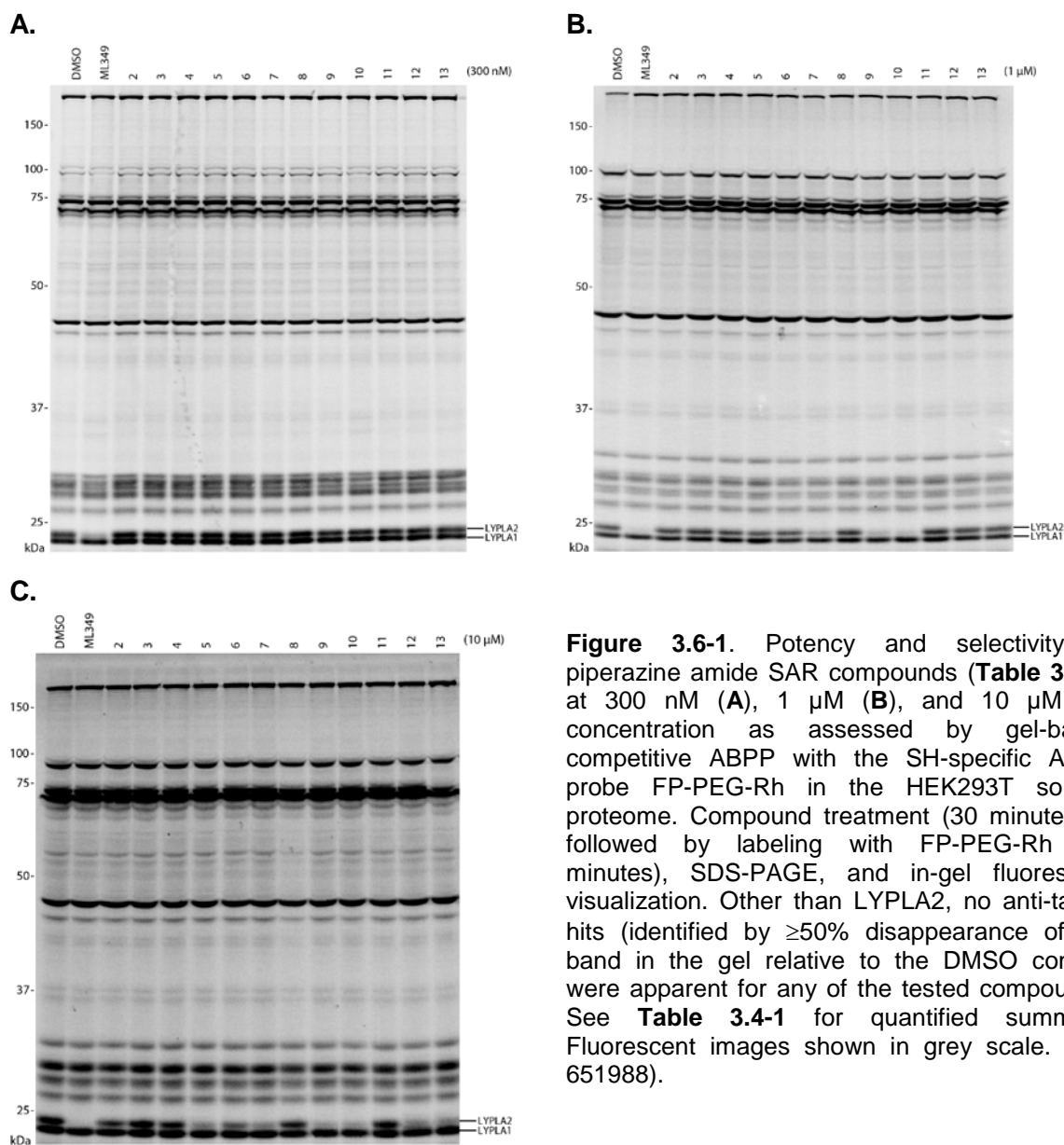


Figure 3.6-1. Potency and selectivity of piperazine amide SAR compounds (**Table 3.4-1**) at 300 nM (**A**), 1 μ M (**B**), and 10 μ M (**C**) concentration as assessed by gel-based competitive ABPP with the SH-specific ABPP probe FP-PEG-Rh in the HEK293T soluble proteome. Compound treatment (30 minutes) is followed by labeling with FP-PEG-Rh (30 minutes), SDS-PAGE, and in-gel fluorescent visualization. Other than LYPLA2, no anti-target hits (identified by $\geq 50\%$ disappearance of the band in the gel relative to the DMSO control) were apparent for any of the tested compounds. See **Table 3.4-1** for quantified summary. Fluorescent images shown in grey scale. (AID 651988).

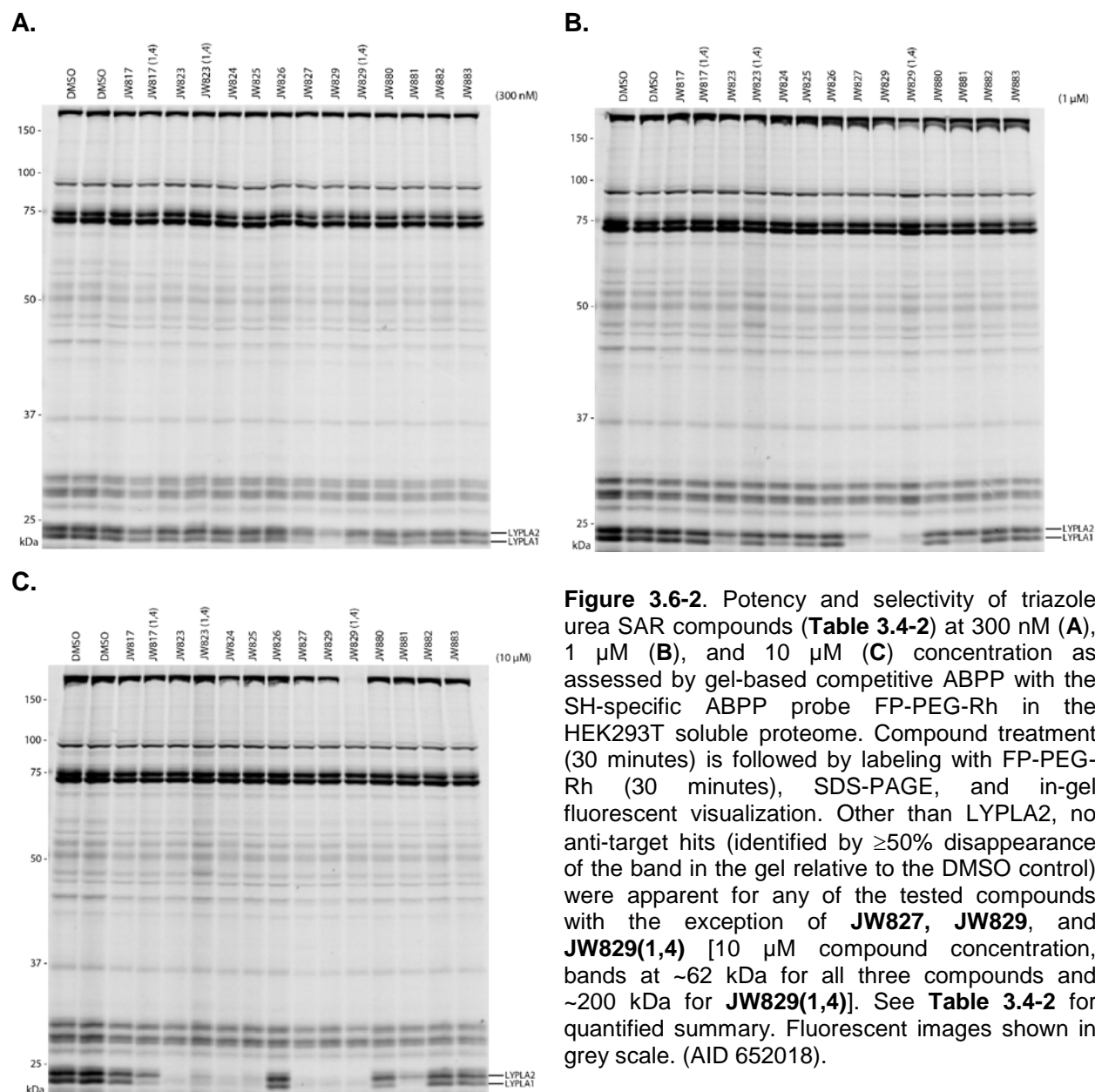


Figure 3.6-2. Potency and selectivity of triazole urea SAR compounds (**Table 3.4-2**) at 300 nM (**A**), 1 μ M (**B**), and 10 μ M (**C**) concentration as assessed by gel-based competitive ABPP with the SH-specific ABPP probe FP-PEG-Rh in the HEK293T soluble proteome. Compound treatment (30 minutes) is followed by labeling with FP-PEG-Rh (30 minutes), SDS-PAGE, and in-gel fluorescent visualization. Other than LYPLA2, no anti-target hits (identified by $\geq 50\%$ disappearance of the band in the gel relative to the DMSO control) were apparent for any of the tested compounds with the exception of **JW827**, **JW829**, and **JW829(1,4)** [10 μ M compound concentration, bands at ~ 62 kDa for all three compounds and ~ 200 kDa for **JW829(1,4)**]. See **Table 3.4-2** for quantified summary. Fluorescent images shown in grey scale. (AID 652018).

ABPP-SILAC: To more comprehensively identify potential anti-targets, we utilized an advanced quantitative mass spectrometry (MS)-based platform termed competitive ABPP-SILAC (**Figure 3.6-6**, left panel). Competitive ABPP-SILAC [12] combines competitive ABPP [16] with stable isotope labeling of cells (SILAC) [27], and allows for precise quantitation of enzyme inhibition by calculating the isotopic ratios of peptides from inhibitor-treated and control cells. We estimate that the sensitivity of a standard LC-MS/MS based ABPP-SILAC assay is at least 10-fold higher than our gel-based assays (0.00005% of the total cell proteome, or 20 copies per cell). As such,

this method offers more sensitive detection of low abundance SHs for a comprehensive selectivity analysis.

In vitro analysis: BW5147-derived murine T-cell hybridoma cells were cultured in 'light' medium (with $^{12}\text{C}_6^{14}\text{N}_2$ -lysine and $^{12}\text{C}_6^{14}\text{N}_4$ -arginine) or 'heavy' medium (with $^{13}\text{C}_6^{15}\text{N}_2$ -lysine [+8] and $^{13}\text{C}_6^{15}\text{N}_4$ -arginine [+10]). After 5-10 passages, near-complete (>97%) enrichment is achieved. Cells were harvested, homogenized, and the soluble and membrane fractions isolated. The light proteomes were treated with 1 μM ML349 (AID 651981) and heavy proteomes were treated with DMSO. After 30 minutes, proteomes were treated with the affinity-tagged SH-specific probe FP-PEG-biotin [12]. Light (ML349-treated) and heavy (DMSO-treated) fractions were then mixed (1:1 w/w light/heavy), enriched with avidin, digested on-bead with trypsin, and analyzed by MudPIT LC-MS/MS [28, 29] using an LTQ-Orbitrap instrument. Light and heavy signals were quantified from parent ion peaks (MS1) and the corresponding proteins identified from product ion profiles (MS2) using the ProLucid search algorithm and filtered using DTASelect (programs available at: <http://fields.scripps.edu/researchtools.php>). The depicted bar graph represents the average ratios of light/heavy tryptic peptides for each of the SHs identified. Enzymes susceptible to inhibition upon compound treatment would be expected to have light/heavy ratios significantly less than one, while uninhibited enzymes would be expected to have a ratio close to one. The results (**Figure 3.6-3**, right panel) indicate that ML349 displays high selectivity for mouse LYPLA2 (arrow), blocking >95% of activity *in vitro*, while not affecting the activity of ~30 other SHs, including close homolog LYPLA1 (arrow).

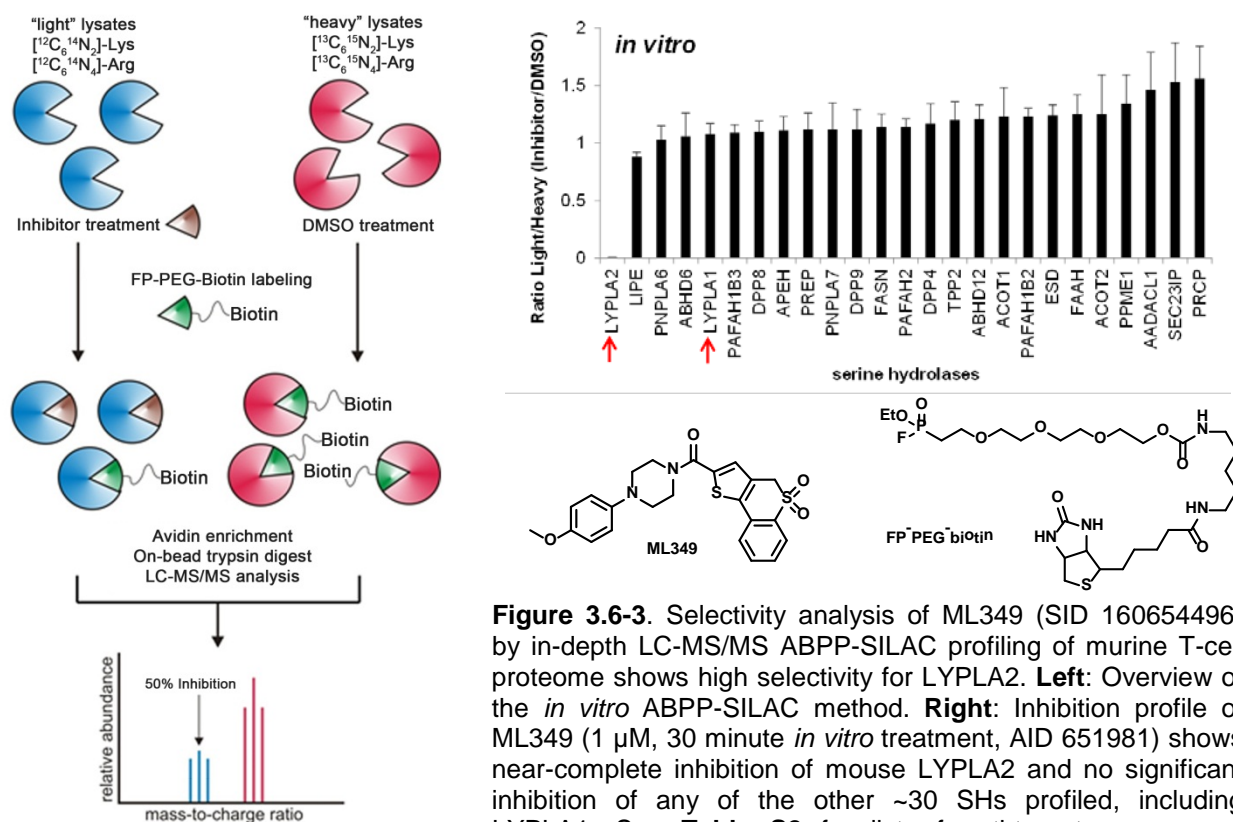


Figure 3.6-3. Selectivity analysis of ML349 (SID 160654496) by in-depth LC-MS/MS ABPP-SILAC profiling of murine T-cell proteome shows high selectivity for LYPLA2. **Left:** Overview of the *in vitro* ABPP-SILAC method. **Right:** Inhibition profile of ML349 (1 μM , 30 minute *in vitro* treatment, AID 651981) shows near-complete inhibition of mouse LYPLA2 and no significant inhibition of any of the other ~30 SHs profiled, including LYPLA1. See **Table S2** for list of anti-target names and abbreviations.

penetration, and likely rapid metabolism in the liver. The use of kinetically-tuned ABPP probes (FP-PEG-Rh and NHU5) were instrumental for the direct confirmation of target engagement this reversible (**Section 3.3**) inhibitor [12]. High selectivity was confirmed for ML349 by gel-based competitive ABPP *in vitro* (**Section 3.6**) and *in vivo* (**Section 3.5**), as well as by more in-depth LC-MS/MS ABPP-SILAC *in vitro* and *in situ* (**Section 3.6**). The probe is soluble in serum-containing buffer at 8.6 μM , well above its active *in situ* concentration (5 μM), and exhibits chemical stability as assessed by GSH reactivity assays (**Section 2.2**) and its successful application in living systems (**Section 3.5**). Taken together, these findings suggest that ML349 will be a highly successful probe for biochemical investigation of human and/or mouse LYPLA2.

4.1 Comparison to existing art and how the new probe is an improvement

No selective LYPLA2 inhibitors have been reported in the literature (PubChem and Google searches for [(LYPLA2 OR APT2 OR lysophospholipase 2 OR Acyl protein thioesterase) AND inhibit*]). As such, ML349 represents the first selective chemical tool for investigation of this uncharacterized enzyme.

4.2 Mechanism of Action Studies

ML349 does not possess any obvious electrophilic moieties for covalent modification of LYPLA2. Reversibility of enzyme inhibition was confirmed by gel filtration studies (AID 651987, **Section 3.3**). Owing to competition with active-site directed activity-based FP and triazole urea probes [12], it can be inferred that ML349 interacts with the active site of LYPLA2.

4.3 Planned Future Studies

We anticipate using ML349 to investigate the endogenous role(s) of LYPLA2 through global proteomic, palmitoylation [1, 11] and metabolomic profiling [30]. In these studies, dual LYPLA1/LYPLA2 inhibitor ML211 and LYPLA1-selective inhibitor ML348 will serve as invaluable controls.

5 References

1. Martin, B.R. and B.F. Cravatt, *Large-scale profiling of protein palmitoylation in mammalian cells*. Nat. Methods, 2009. **6**(2): p. 135-8.
2. Dekker, F.J., et al., *Small-molecule inhibition of APT1 affects Ras localization and signaling*. Nat. Chem. Biol., 2010. **6**(6): p. 449-56.
3. Smotrys, J.E. and M.E. Linder, *Palmitoylation of intracellular signaling proteins: regulation and function*. Annu. Rev. Biochem., 2004. **73**: p. 559-87.
4. Magee, A.I., et al., *Release of fatty acids from virus glycoproteins by hydroxylamine*. Biochim. Biophys. Acta, 1984. **798**(2): p. 156-66.
5. Rose, J.K., G.A. Adams, and C.J. Gallione, *The presence of cysteine in the cytoplasmic domain of the vesicular stomatitis virus glycoprotein is required for palmitate addition*. Proc. Natl. Acad. Sci. U. S. A., 1984. **81**(7): p. 2050-4.

6. Willumsen, B.M., et al., *Novel determinants of H-Ras plasma membrane localization and transformation*. *Oncogene*, 1996. **13**(9): p. 1901-9.
7. Duncan, J.A. and A.G. Gilman, *A cytoplasmic acyl-protein thioesterase that removes palmitate from G protein alpha subunits and p21(RAS)*. *J. Biol. Chem.*, 1998. **273**(25): p. 15830-7.
8. Sugimoto, H., H. Hayashi, and S. Yamashita, *Purification, cDNA cloning, and regulation of lysophospholipase from rat liver*. *J. Biol. Chem.*, 1996. **271**(13): p. 7705-11.
9. Hirano, T., et al., *Thioesterase activity and subcellular localization of acylprotein thioesterase 1/lysophospholipase 1*. *Biochim. Biophys. Acta*, 2009. **1791**(8): p. 797-805.
10. Toyoda, T., H. Sugimoto, and S. Yamashita, *Sequence, expression in Escherichia coli, and characterization of lysophospholipase II*. *Biochim. Biophys. Acta*, 1999. **1437**(2): p. 182-93.
11. Martin, B.R., et al., *Global profiling of dynamic protein palmitoylation*. *Nat. Methods*, 2012. **9**(1): p. 84-9.
12. Adibekian, A., et al., *Confirming target engagement for reversible inhibitors in vivo by kinetically tuned activity-based probes*. *J. Am. Chem. Soc.*, 2012. **134**(25): p. 10345-8.
13. Biel, M., et al., *Synthesis and evaluation of acyl protein thioesterase 1 (APT1) inhibitors*. *Chemistry*, 2006. **12**(15): p. 4121-43.
14. Deck, P., et al., *Development and biological evaluation of acyl protein thioesterase 1 (APT1) inhibitors*. *Angew. Chem. Int. Ed. Engl.*, 2005. **44**(31): p. 4975-80.
15. Jessani, N., et al., *Enzyme activity profiles of the secreted and membrane proteome that depict cancer cell invasiveness*. *Proc. Natl. Acad. Sci. U. S. A.*, 2002. **99**(16): p. 10335-40.
16. Leung, D., et al., *Discovering potent and selective reversible inhibitors of enzymes in complex proteomes*. *Nat. Biotechnol.*, 2003. **21**(6): p. 687-91.
17. Bachovchin, D.A., et al., *Identification of selective inhibitors of uncharacterized enzymes by high-throughput screening with fluorescent activity-based probes*. *Nat. Biotechnol.*, 2009. **27**(4): p. 387-94.
18. Heal, W.P., T.H. Dang, and E.W. Tate, *Activity-based probes: discovering new biology and new drug targets*. *Chem. Soc. Rev.*, 2011. **40**(1): p. 246-57.
19. Lenz, T., J.J. Fischer, and M. Dreger, *Probing small molecule-protein interactions: A new perspective for functional proteomics*. *J. Proteomics*, 2011. **75**(1): p. 100-15.
20. Li, N., H.S. Overkleeft, and B.I. Florea, *Activity-based protein profiling: an enabling technology in chemical biology research*. *Curr. Opin. Chem. Biol.*, 2012. **16**(1-2): p. 227-33.
21. Nomura, D.K., M.M. Dix, and B.F. Cravatt, *Activity-based protein profiling for biochemical pathway discovery in cancer*. *Nat. Rev. Cancer*, 2010. **10**(9): p. 630-8.
22. Chiang, K.P., et al., *An enzyme that regulates ether lipid signaling pathways in cancer annotated by multidimensional profiling*. *Chem. Biol.*, 2006. **13**(10): p. 1041-50.
23. Long, J.Z., et al., *Selective blockade of 2-arachidonoylglycerol hydrolysis produces cannabinoid behavioral effects*. *Nat. Chem. Biol.*, 2009. **5**(1): p. 37-44.
24. Adibekian, A., et al., *Click-generated triazole ureas as ultrapotent in vivo-active serine hydrolase inhibitors*. *Nat. Chem. Biol.*, 2011. **7**(7): p. 469-78.
25. Hsu, K.L., et al., *DAGLbeta inhibition perturbs a lipid network involved in macrophage inflammatory responses*. *Nat. Chem. Biol.*, 2012. **8**(12): p. 999-1007.
26. Bachovchin, D.A., et al., *Superfamily-wide portrait of serine hydrolase inhibition achieved by library-versus-library screening*. *Proc. Natl. Acad. Sci. U. S. A.* 2010. **107**(49): p 20941-6.
27. Ong, S.E., et al., *Stable isotope labeling by amino acids in cell culture, SILAC, as a simple and accurate approach to expression proteomics*. *Mol. Cell. Proteomics*, 2002. **1**(5): p. 376-86.

28. Washburn, M.P., D. Wolters, and J.R. Yates, 3rd, *Large-scale analysis of the yeast proteome by multidimensional protein identification technology*. Nat. Biotechnol., 2001. **19**(3): p. 242-7.
29. Wolters, D.A., M.P. Washburn, and J.R. Yates, 3rd, *An automated multidimensional protein identification technology for shotgun proteomics*. Anal. Chem., 2001. **73**(23): p. 5683-90.
30. Harkewicz, R. and E.A. Dennis, *Applications of mass spectrometry to lipids and membranes*. Annu. Rev. Biochem., 2011. **80**: p. 301-25.

6 Supplemental Information for ML349 Probe Report

Figure S1: First Round Secondary Screening: Competitive-ABPP profiling with recombinant human (rh) LYPLA2 and endogenous mouse LYPLA1 and LYPLA2 in the mouse brain soluble proteome with 20 μ M test compound (30 minutes) and the SH-specific FP-Rh ABPP probe (2 μ M, 30 minutes). See **Table S1** for quantified results and compound SIDs and structures. Fluorescent images shown in grey scale. (AID 652029).

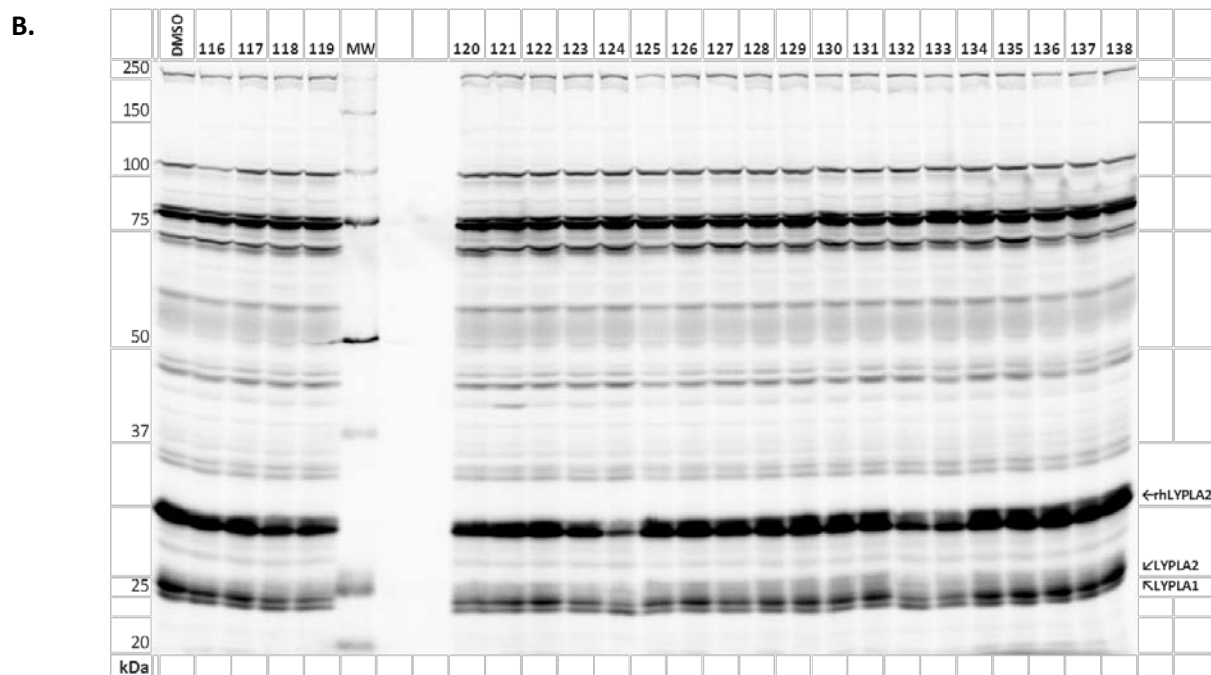
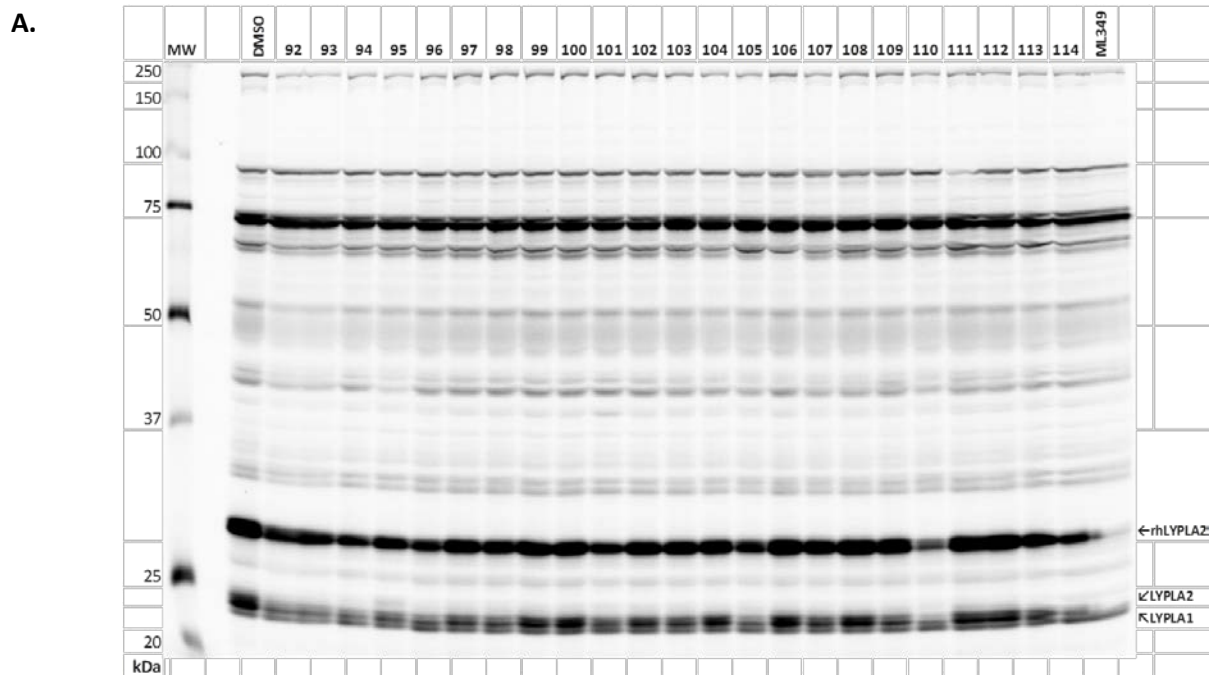
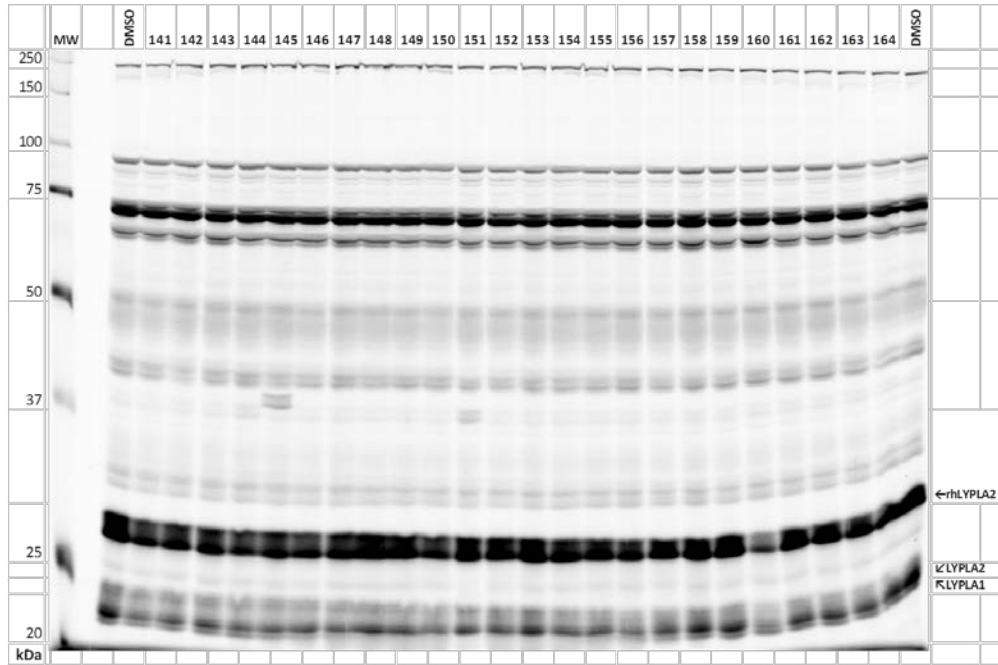


Figure S1. Continued.

C.



D.

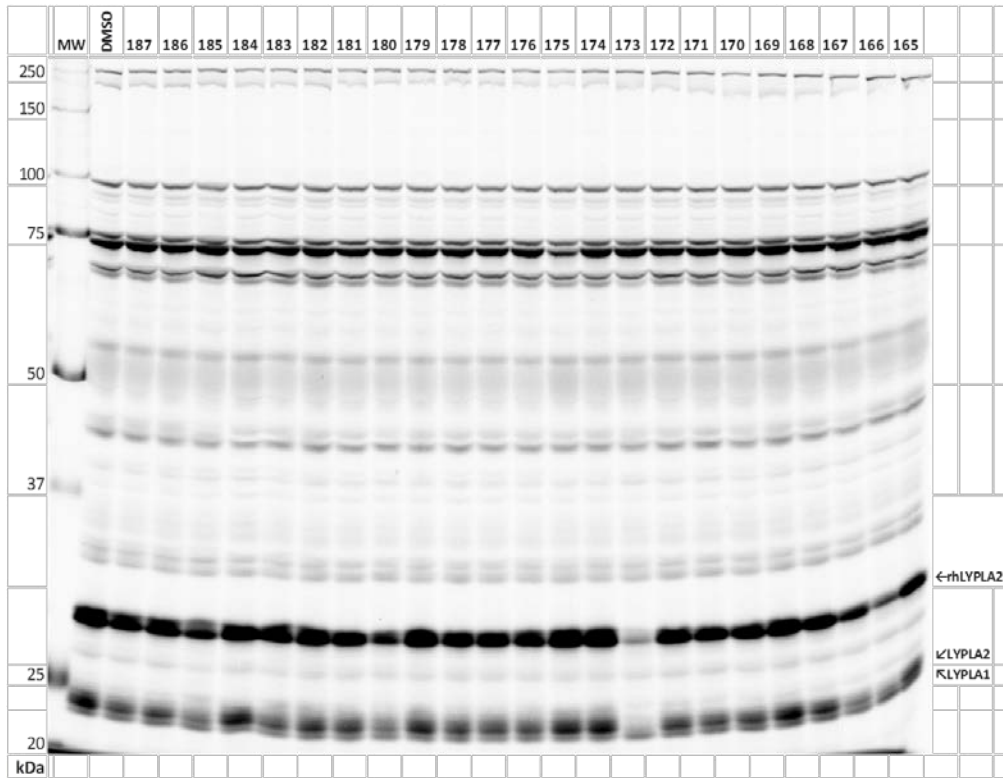
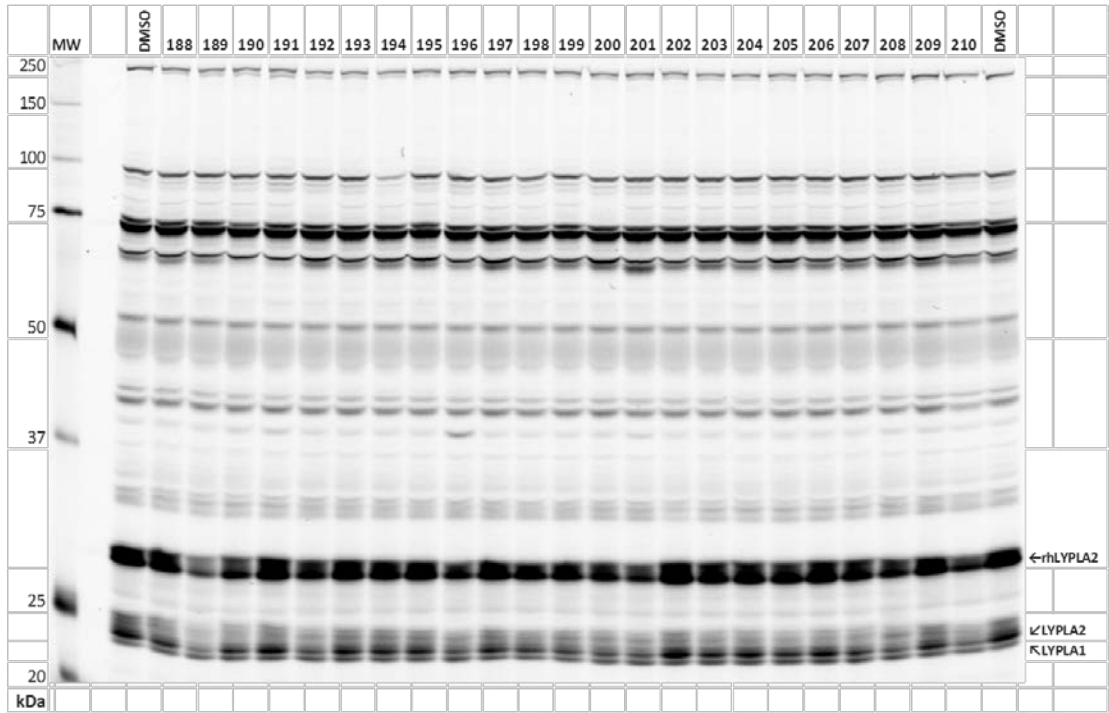


Figure S1. Continued.

E.



F.

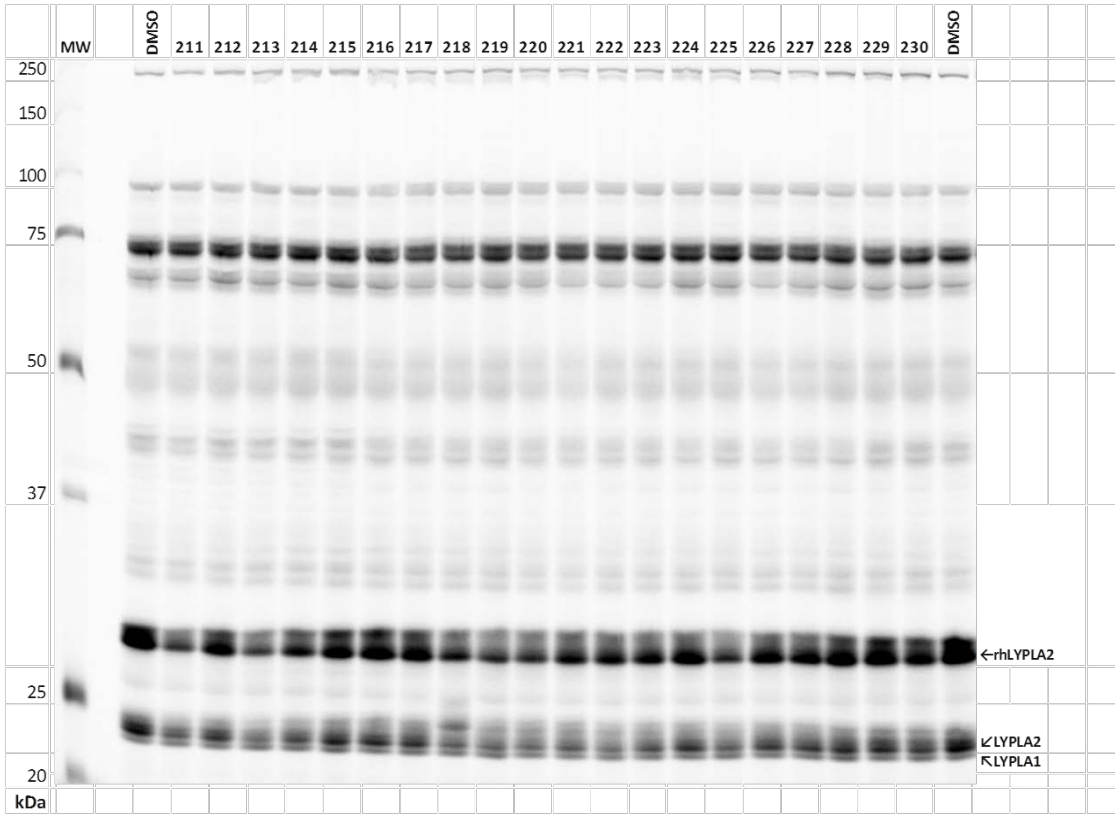


Figure S1. Continued.

G.

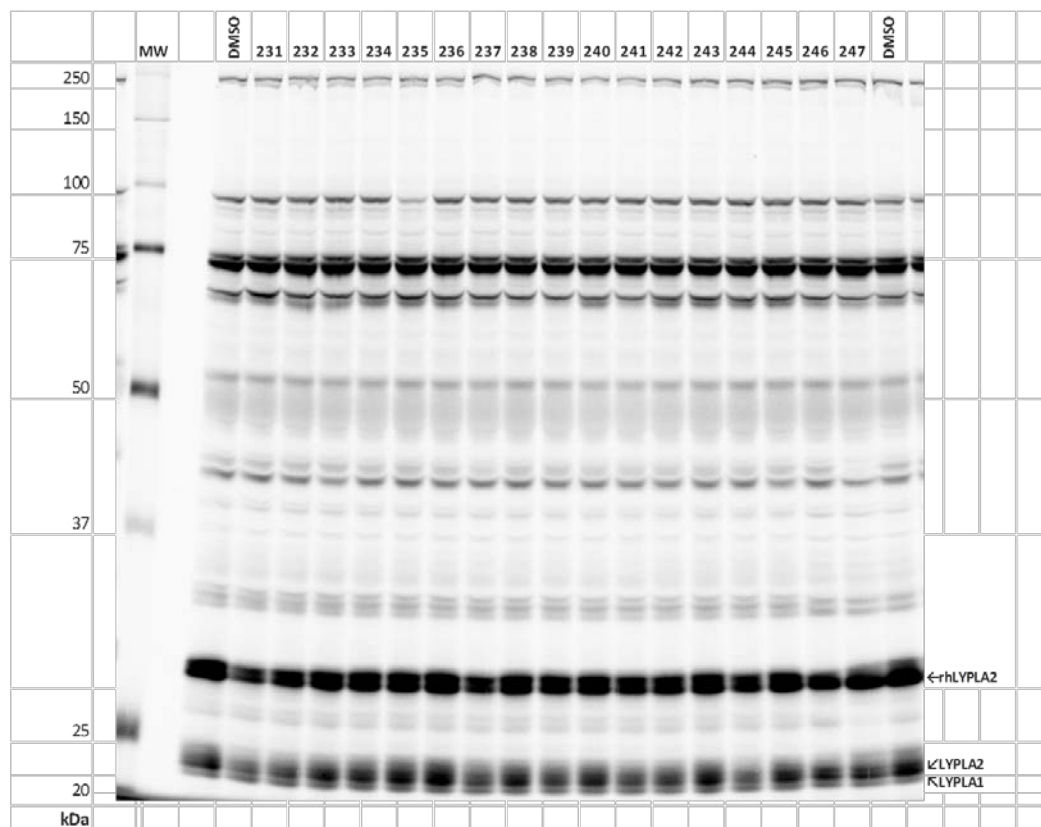
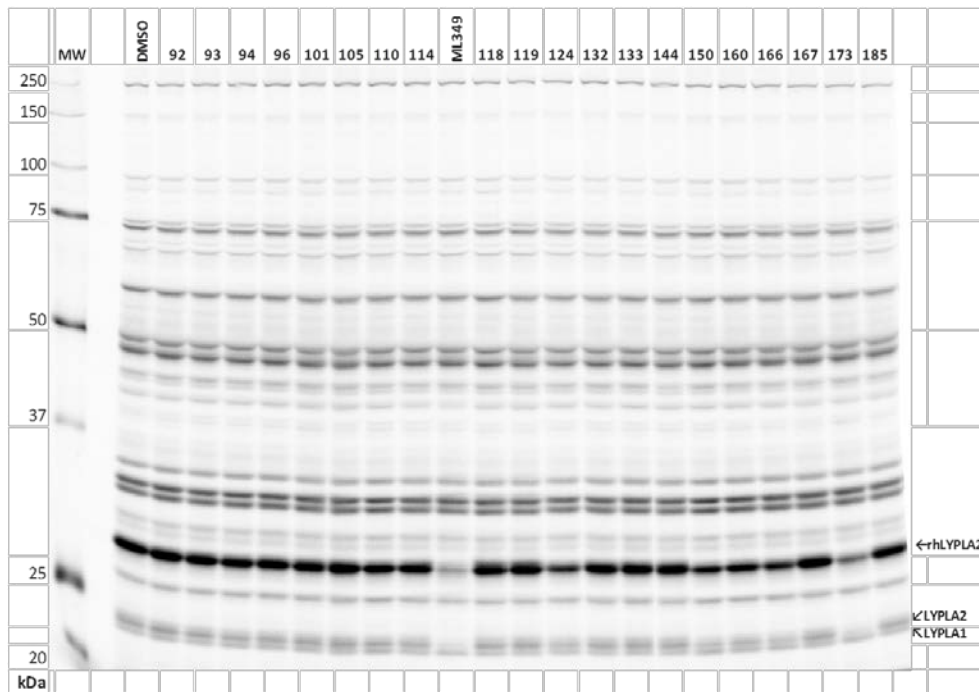


Figure S2: Second Round Secondary Screening: Competitive-ABPP profiling with recombinant human (rh) LYPLA2 and endogenous mouse LYPLA1 and LYPLA2 in the mouse brain soluble proteome with 10 μ M test compound (30 minutes) and the SH-specific FP-Rh ABPP probe (2 μ M, 30 minutes). See **Table S1** for quantified results and compound SIDs and structures. Fluorescent images shown in grey scale. (AID 652030).

A.



B.

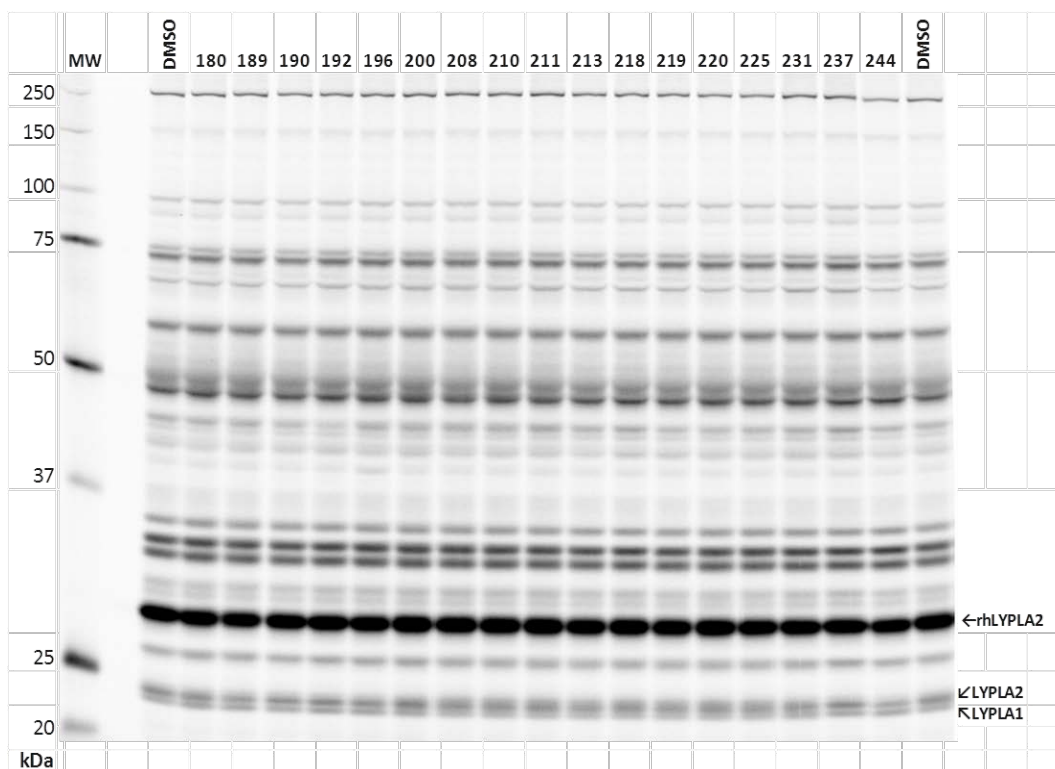
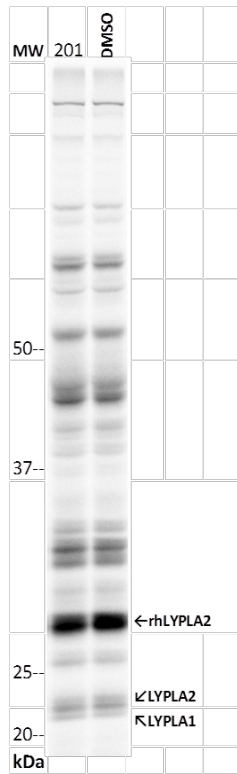


Figure S2. Continued.

C.



D.

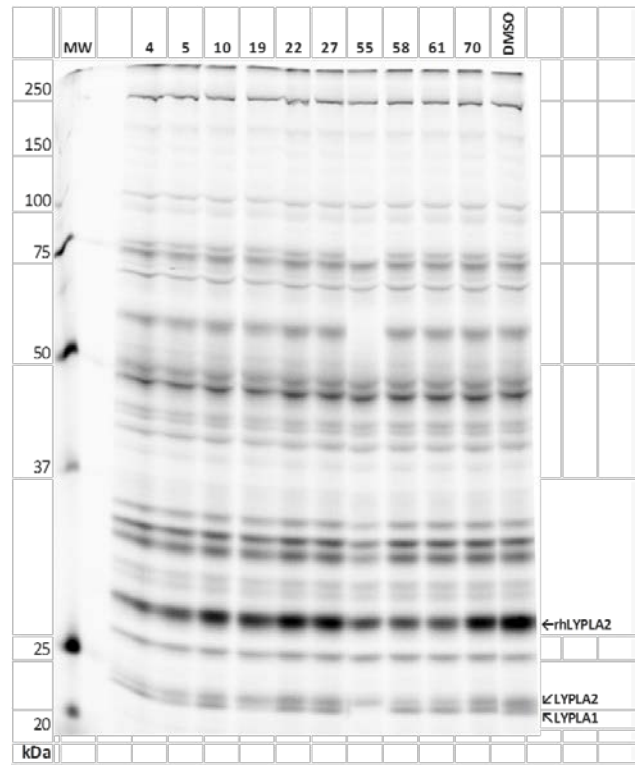
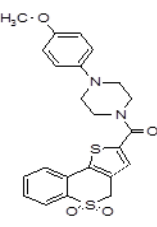
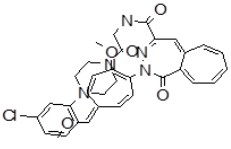
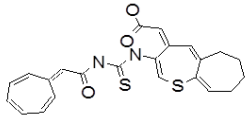
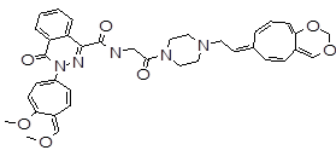
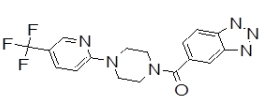
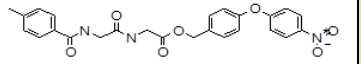
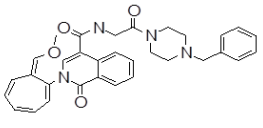
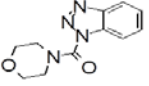
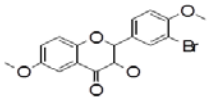
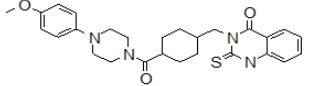
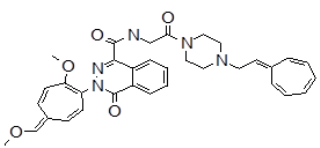
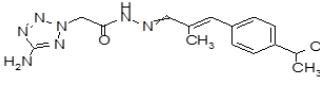
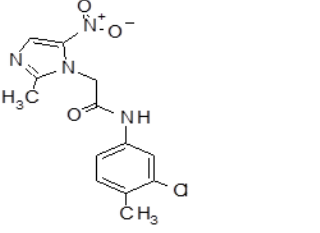
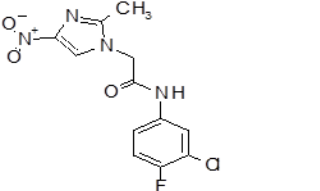
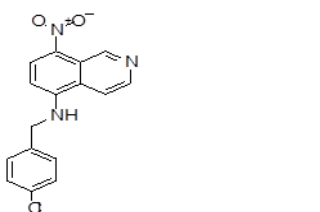
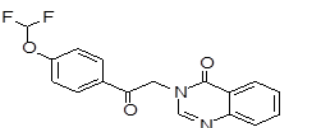
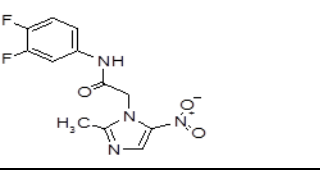
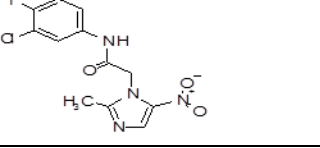
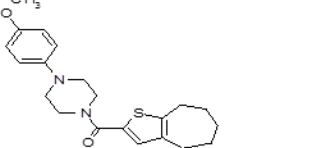
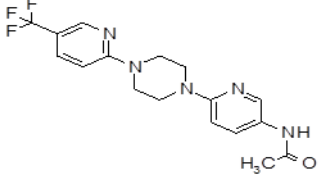
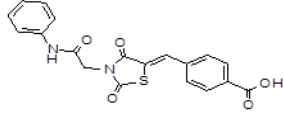
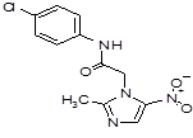
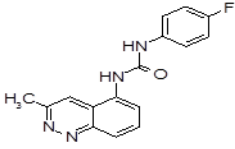
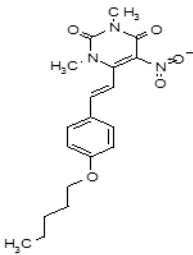
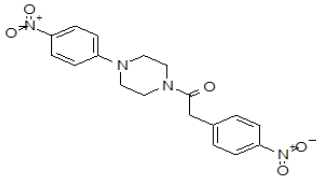
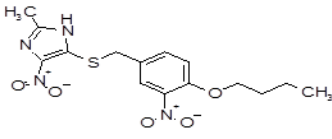
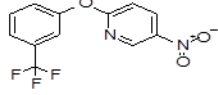
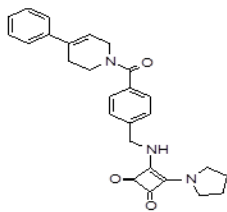
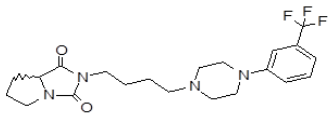
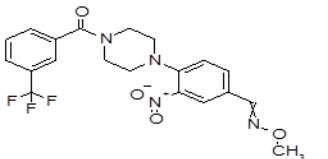
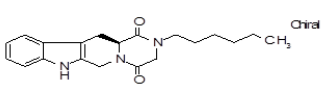
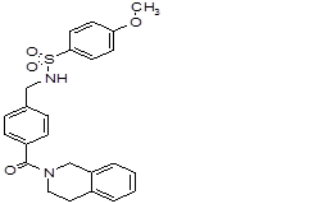
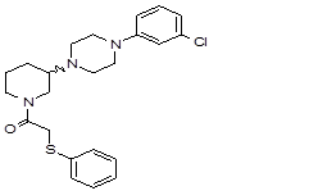
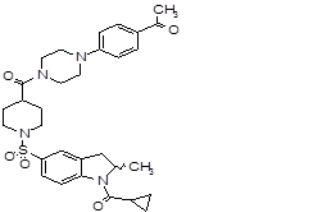
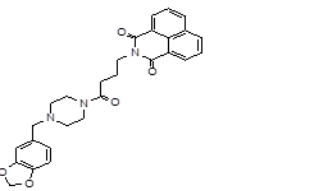
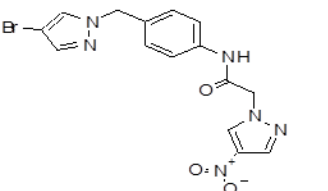


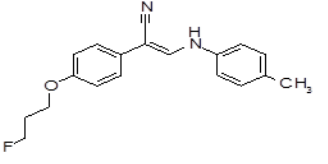
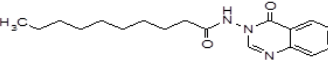
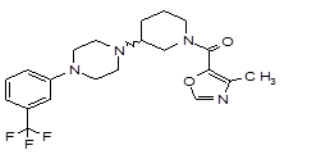
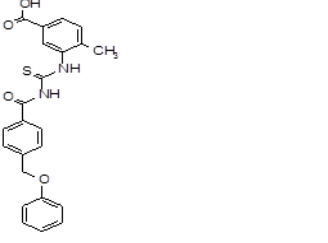
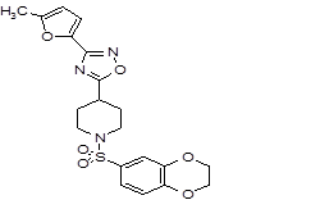
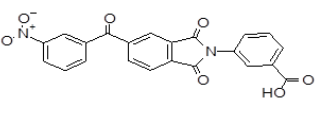
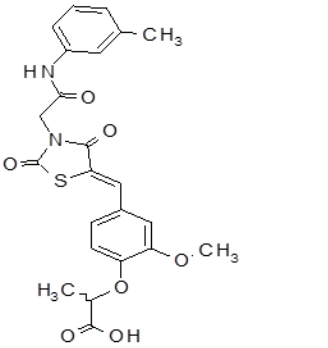
Table S1. Compounds tested by gel-based competitive ABPP Secondary Screening (**Figures S1** and **S2**)

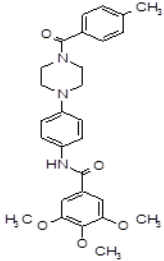
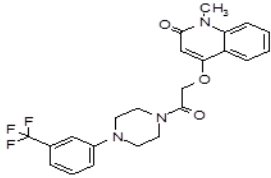
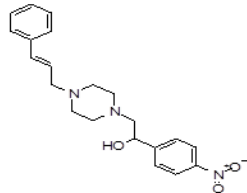
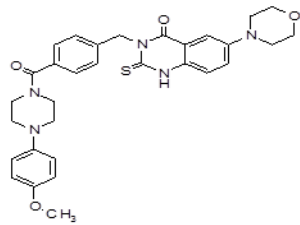
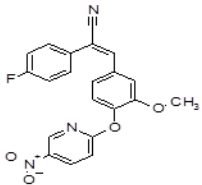
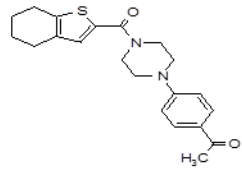
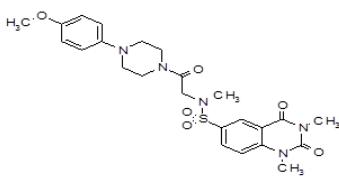
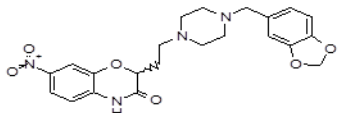
Cpd #	SRID	SID	CID	Structure	% INH rhLYPLA2 (20 μ M) AID 652029; AID 493105	% INH rhLYPLA2 (10 μ M) AID 652030	% INH emLYPLA2 (10 μ M) AID 652030	% INH emLYPLA1 (10 μ M) AID 652030
ML349	SR- 01000775306 -2	92709328	16193817		100%	79%	74%	25%
4	SR- 01000544381 -2	49715467	24789646		61%	52%	41%	33%
5	SR- 01000454606 -2	49640730	1130125		34%	32%	43%	34%
10	SR- 01000544853 -2	24810381	16193079		50%	26%	23%	0%
19	SR- 01000854272 -1	57261525	16297767		32%	26%	35%	40%
22	SR- 01000679356 -1	17414052	2953598		41%	12%	7%	0%
27	SR- 01000543175 -2	24781868	16187671		39%	14%	15%	0%
55	SR- 01000625310 -1	7974398	735660		76%	47%	54%	103%
58	SR- 01000712266 -1	14728505	6917582		51%	47%	55%	23%
61	SR- 01000663277 -1	4245654	3240101		45%	47%	44%	16%

70	SR- 01000544533 -2	49730654	22334024		30%	18%	15%	0%
92	SR- 01000759830 -2	92709318	948192		69%	2%	0%	0%
93	SR- 01000457406 -3	92709254	738164		67%	8%	8%	0%
94	SR- 01000207125 -3	92709240	2843709		70%	10%	15%	0%
95	SR- 01000062699 -3	92709230	4880770		49%	NT	NT	NT
96	SR- 01000819662 -2	92709358	7628255		70%	7%	8%	5%
97	SR- 01000815302 -2	92709357	707079		44%	NT	NT	NT
98	SR- 01000814041 -2	92709355	707134		49%	NT	NT	NT
99	SR- 01000859016 -2	92709376	8294576		32%	NT	NT	NT

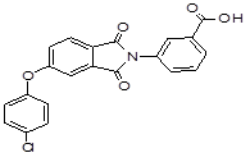
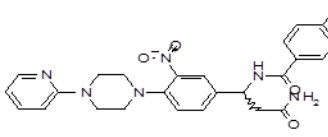
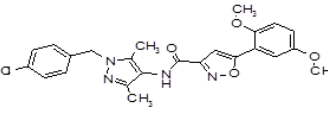
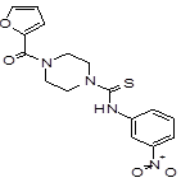
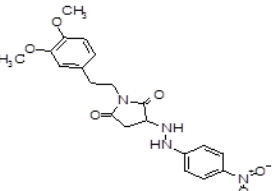
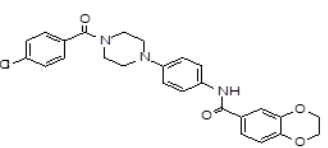
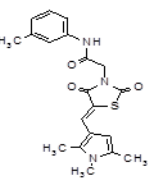
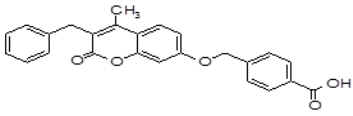
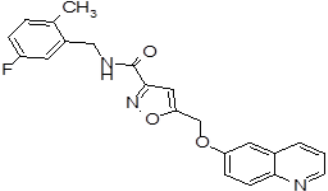
100	SR-01000643300-3	92709274	2741630		27%	NT	NT	NT
101	SR-01000811885-2	92709354	1810599		63%	8%	8%	7%
102	SR-01000814976-2	92709356	753324		34%	NT	NT	NT
103	SR-01000767921-2	92709324	6409921		43%	NT	NT	NT
104	SR-01000081889-3	92709236	22330954		36%	NT	NT	NT
105	SR-01000201553-3	92709239	2837966		70%	0%	0%	0%
106	SR-01000773342-2	92709326	3658974		20%	NT	NT	NT
107	SR-01000773509-2	92709327	286874		47%	NT	NT	NT
108	SR-01000100094-3	92709237	16193979		21%	NT	NT	NT

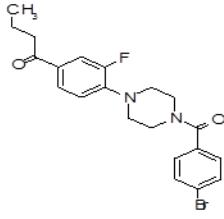
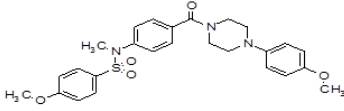
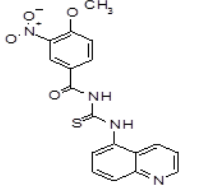
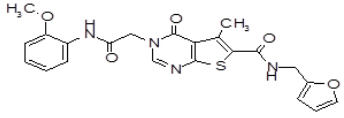
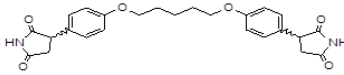
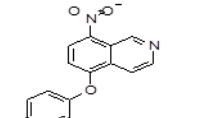
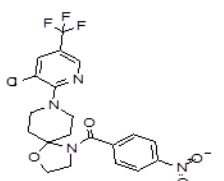
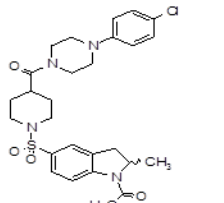
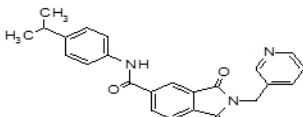
109	SR-01000803679-2	92709348	3565378		44%	NT	NT	NT
110	SR-01000678819-2	92709284	2768219		88%	14%	14%	14%
111	SR-01000805308-2	92709350	7003666		35%	NT	NT	NT
112	SR-01000714245-2	92709299	12005305		28%	NT	NT	NT
113	SR-01000797319-2	92709341	24791323		48%	NT	NT	NT
114	SR-01000807919-2	92709352	24792060		70%	10%	19%	18%
116	SR-01000443086-3	92709252	2872850		25%	NT	NT	NT
117	SR-01000701446-2	92709290	997434		20%	NT	NT	NT

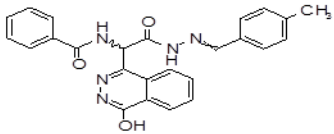
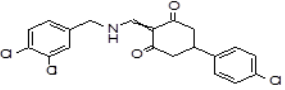
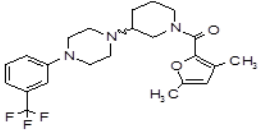
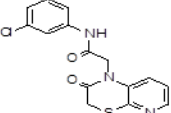
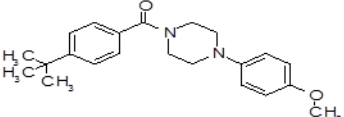
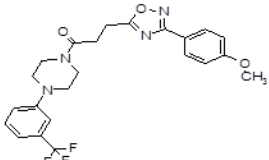
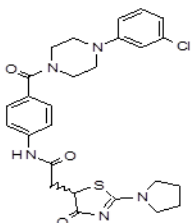
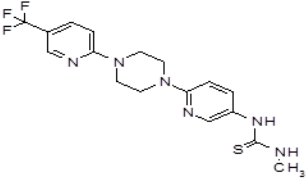
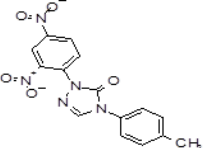
118	SR-01000666775-2	92709277	6036769		52%	5%	13%	17%
119	SR-01000732660-2	92709306	1649169		52%	4%	12%	28%
120	SR-01000802662-2	92709347	24817537		46%	NT	NT	NT
121	SR-01000834300-2	92709370	1304219		23%	NT	NT	NT
122	SR-01000331369-3	92709250	646874		9%	NT	NT	NT
123	SR-01000360756-3	92709251	3091522		45%	NT	NT	NT
124	SR-01000845983-2	92709371	6520605		80%	58%	37%	28%

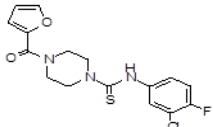
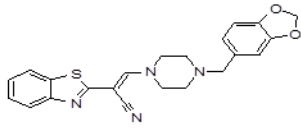
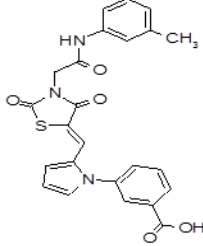
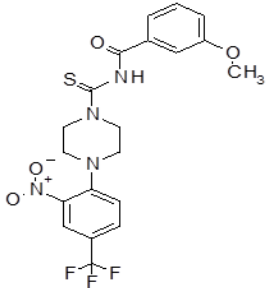
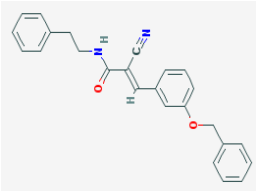
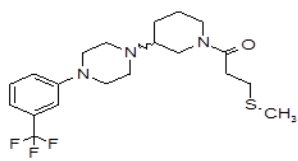
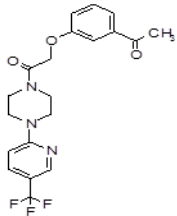
125	SR- 01000833730 -2	92709369	2958977		35%	NT	NT	NT
126	SR- 01000621197 -2	92709268	3240891		15%	NT	NT	NT
127	SR- 01000223822 -3	92709241	5344976		36%	NT	NT	NT
128	SR- 01000756517 -2	92709316	16193498		33%	NT	NT	NT
129	SR- 01000705143 -2	92709293	5663990		19%	NT	NT	NT
130	SR- 01000291611 -3	92709247	1245607		28%	NT	NT	NT
131	SR- 01000735614 -2	92709308	16194493		14%	NT	NT	NT
132	SR- 01000749021 -2	92709311	3721644		61%	9%	21%	27%

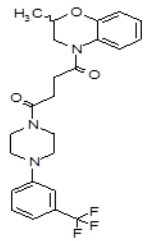
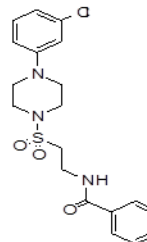
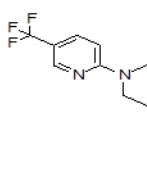
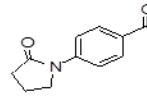
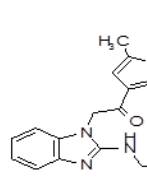
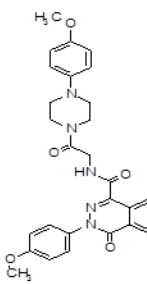
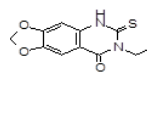
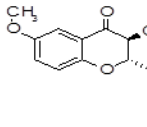
133	SR- 01000742048 -2	92709310	4173716		60%	8%	16%	19%
134	SR- 01000793455 -2	92709339	24791651		12%	NT	NT	NT
135	SR- 01000446197 -3	92709253	16193281		12%	NT	NT	NT
136	SR- 01000078450 -3	92709235	3965305		1%	NT	NT	NT
137	SR- 01000282109 -3	92709245	9552010		20%	NT	NT	NT
138	SR- 01000757786 -2	92709317	1306183		3%	NT	NT	NT
141	SR- 01000780012 -2	92709330	16746106		45%	NT	NT	NT
142	SR- 01000737809 -2	92709309	15988659		37%	NT	NT	NT
143	SR- 01000797748 -2	92709344	984432		34%	NT	NT	NT

144	SR-01000754130-2	92709315	1297453		55%	7%	11%	25%
145	SR-01000780744-2	92709331	16746244		37%	NT	NT	NT
146	SR-01000601378-2	92709261	3236433		45%	NT	NT	NT
147	SR-01000275474-3	92709244	1295275		36%	NT	NT	NT
148	SR-01000293957-3	92709248	4922434		17%	NT	NT	NT
149	SR-01000676688-2	92709282	1254489		24%	NT	NT	NT
150	SR-01000702900-2	92709291	2252839		60%	51%	40%	9%
151	SR-01000729542-2	92709305	978403		24%	NT	NT	NT
152	SR-01000753813-2	92709314	16190237		31%	NT	NT	NT

153	SR- 01000469930 -3	92709255	613159		8%	NT	NT	NT
154	SR- 01000752432 -2	92709313	2974294		36%	NT	NT	NT
155	SR- 01000284867 -3	92709246	1254617		38%	NT	NT	NT
156	SR- 01000589819 -3	92709260	3245476		49%	NT	NT	NT
157	SR- 01000733170 -2	92709307	3071136		32%	NT	NT	NT
158	SR- 01000066572 -3	92709232	2570042		12%	NT	NT	NT
159	SR- 01000665583 -2	92709276	1478850		8%	NT	NT	NT
160	SR- 01000786127 -2	92709334	20910602		75%	32%	26%	3%
161	SR- 01000828709 -2	92709366	1026077		26%	NT	NT	NT

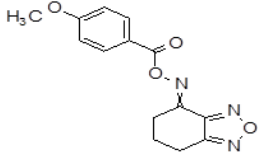
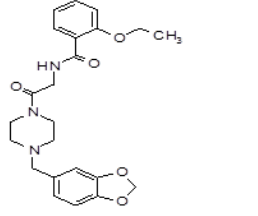
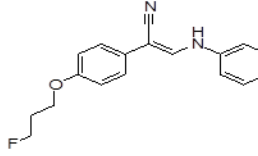
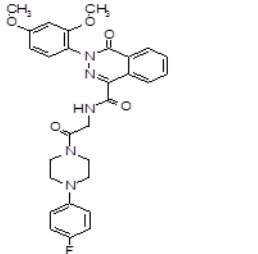
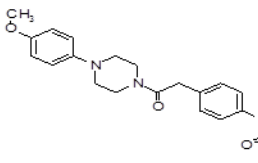
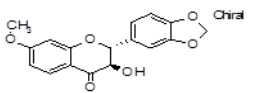
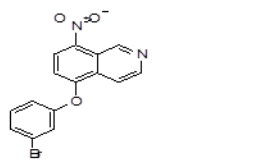
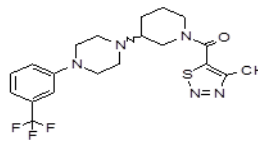
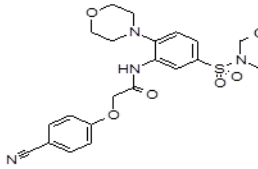
162	SR-01000683355-2	92709287	3462007		28%	NT	NT	NT
163	SR-01000673732-2	92709281	3902161		37%	NT	NT	NT
164	SR-01000824627-2	92709362	24792930		31%	NT	NT	NT
165	SR-01000830441-2	92709367	20889981		46%	NT	NT	NT
166	SR-01000679418-2	92709285	1316101		86%	57%	47%	16%
167	SR-01000662341-2	92709275	3243472		70%	2%	14%	1%
168	SR-01000848981-2	92709373	24981750		38%	NT	NT	NT
169	SR-01000766596-2	92709323	2741788		19%	NT	NT	NT
170	SR-01000801514-2	92709346	3788602		46%	NT	NT	NT

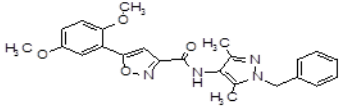
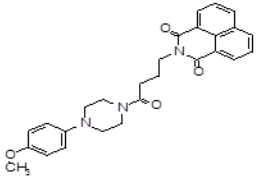
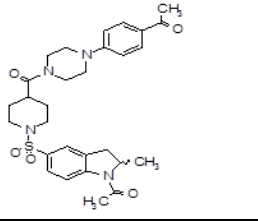
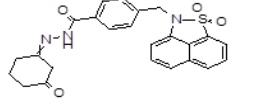
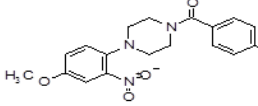
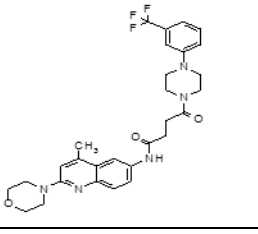
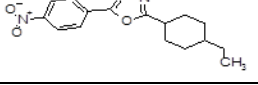
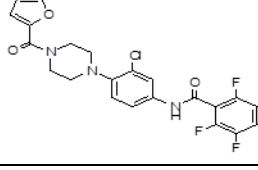
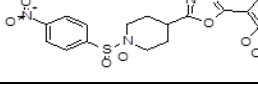
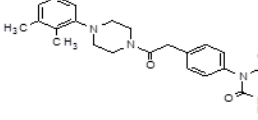
171	SR-01000831430-2	92709368	1840362		47%	NT	NT	NT
172	SR-01000001214-2	92709228	662891		40%	NT	NT	NT
173	SR-01000723100-2	92709303	11839276		94%	66%	77%	17%
174	SR-01000709307-2	92709296	2898999		13%	NT	NT	NT
175	SR-01000715741-2	92709300	6172362		15%	NT	NT	NT
176	SR-01000810886-2	92709353	23724070		49%	NT	NT	NT
177	SR-01000750069-2	92709312	4878098		45%	NT	NT	NT

178	SR-01000793481-2	92709340	22512977		44%	NT	NT	NT
179	SR-01000847861-2	92709372	18582853		20%	NT	NT	NT
180	SR-01000766413-2	92709322	2741775		72%	8%	1%	0%
181	SR-01000797397-2	92709342	3680379		40%	NT	NT	NT
182	SR-01000065907-3	92709231	2999829		29%	NT	NT	NT
183	SR-01000546965-3	92709258	22421608		43%	NT	NT	NT
184	SR-01000560006-3	92709259	3239043		13%	NT	NT	NT
185	SR-01000721481-2	92709301	9548123		63%	20%	31%	13%

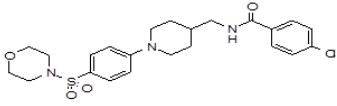
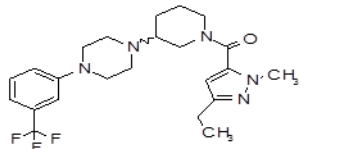
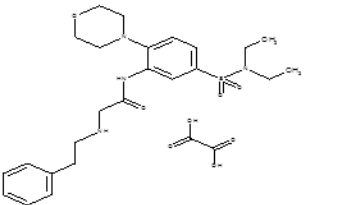
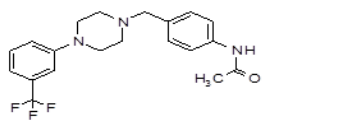
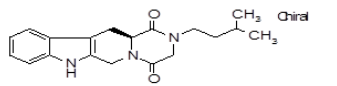
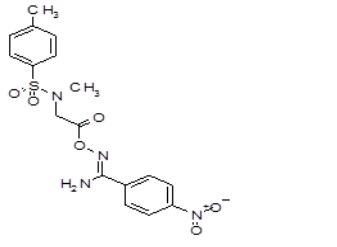
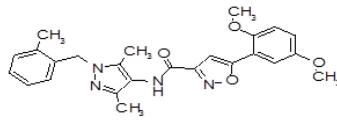
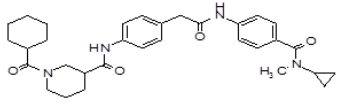
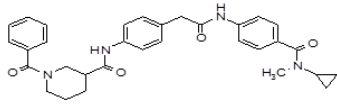
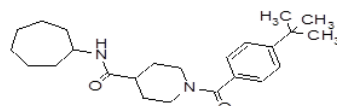
186	SR-01000784484-2	92709333	1086023		38%	NT	NT	NT
187	SR-01000825443-2	92709364	20962749		49%	NT	NT	NT
188	SR-01000608049-2	92709263	5309969		35%	NT	NT	NT
189	SR-01000000093-9	92709227	5213		75%	14%	19%	10%
190	SR-01000686648-2	92709288	1280564		53%	9%	6%	14%
191	SR-01000760123-2	92709319	24747539		16%	NT	NT	NT
192	SR-01000633085-3	92709273	2810354		50%	8%	0%	7%
193	SR-01000850947-2	92709374	16573489		25%	NT	NT	NT
194	SR-01000805263-2	92709349	7003681		38%	NT	NT	NT

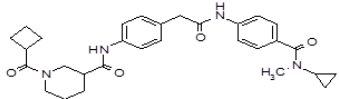
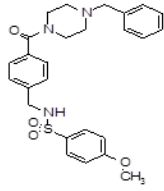
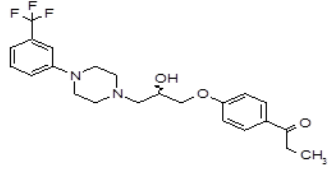
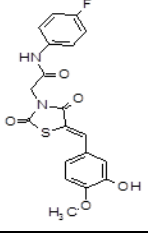
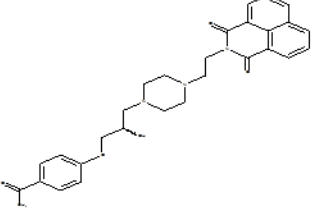
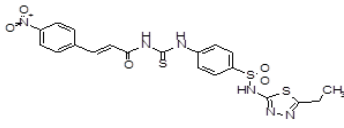
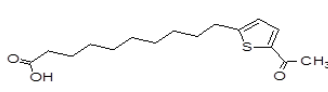
195	SR-01000793099-2	92709337	24789921		25%	NT	NT	NT
196	SR-01000800701-2	92709345	1365399		59%	7%	4%	6%
197	SR-01000630272-3	92709272	5742525		29%	NT	NT	NT
198	SR-01000726885-2	92709304	16195068		47%	NT	NT	NT
199	SR-01000791287-2	92709336	16297726		47%	NT	NT	NT
200	SR-01000667532-2	92709279	1377323		56%	2%	0%	0%
201	SR-01000691545-2	92709289	11839291		64%	4%	13%	0%

202	SR-01000707739-2	92709295	685764		6%	NT	NT	NT
203	SR-01000858430-2	92709375	9204120		39%	NT	NT	NT
204	SR-01000667215-2	92709278	5793288		37%	NT	NT	NT
205	SR-01000544545-3	92709257	22334032		41%	NT	NT	NT
206	SR-01000615990-2	92709267	3236420		28%	NT	NT	NT
207	SR-01000712160-2	92709297	6917421		45%	NT	NT	NT
208	SR-01000066688-3	92709233	2571709		57%	2%	0%	13%
209	SR-01000824673-2	92709363	24791406		28%	NT	NT	NT
210	SR-01000771036-2	92709325	4412828		64%	3%	0%	12%

211	SR-01000122489-3	92709238	3236902		64%	3%	0%	15%
212	SR-01000497226-3	92709256	2926808		32%	NT	NT	NT
213	SR-01000807695-2	92709351	24792905		64%	8%	10%	18%
214	SR-01000713834-2	92709298	3292126		44%	NT	NT	NT
215	SR-01000294241-3	92709249	2973383		20%	NT	NT	NT
216	SR-01000821601-2	92709360	15995172		10%	NT	NT	NT
217	SR-01000705213-2	92709294	4526046		23%	NT	NT	NT
218	SR-01000628221-3	92709271	2162197		50%	5%	0%	18%
219	SR-01000076890-3	92709234	24789599		58%	9%	5%	16%
220	SR-01000705033-2	92709292	6621246		56%	4%	0%	14%

221	SR-01000863954-2	92709380	44142715		45%	NT	NT	NT
222	SR-01000864098-2	92709381	44142749		46%	NT	NT	NT
223	SR-01000864120-2	92709382	44142729		45%	NT	NT	NT
224	SR-01000680078-2	92709286	2768222		29%	NT	NT	NT
225	SR-01000825835-2	92709365	3597028		61%	9%	3%	14%
226	SR-01000764111-2	92709321	24747532		35%	NT	NT	NT
227	SR-01000797649-2	92709343	24818875		37%	NT	NT	NT
228	SR-01000608632-2	92709264	5307683		23%	NT	NT	NT
229	SR-01000790625-2	92709335	15987958		16%	NT	NT	NT
230	SR-01000609441-2	92709265	1316078		34%	NT	NT	NT

231	SR-01000667859-2	92709280	3232214		59%	9%	9%	3%
232	SR-01000824457-2	92709361	24791460		43%	NT	NT	NT
233	SR-01000761248-2	92709320	16239899		16%	NT	NT	NT
234	SR-01000625354-2	92709269	1067937		17%	NT	NT	NT
235	SR-01000783468-2	92709332	6953764		14%	NT	NT	NT
236	SR-01000272989-3	92709243	5923405		0%	NT	NT	NT
237	SR-01000601381-2	92709262	3237838		50%	8%	0%	6%
238	SR-01000863494-2	92709377	44142737		13%	NT	NT	NT
239	SR-01000863646-2	92709378	44142744		34%	NT	NT	NT
240	SR-01000820483-2	92709359	1078732		20%	NT	NT	NT

241	SR-01000863713-2	92709379	44142722		41%	NT	NT	NT
242	SR-01000793441-2	92709338	20854208		38%	NT	NT	NT
243	SR-01000626623-2	92709270	115423		18%	NT	NT	NT
244	SR-01000237880-3	92709242	1343676		50%	16%	24%	15%
245	SR-01000721971-2	92709302	15945738		20%	NT	NT	NT
246	SR-01000775340-2	92709329	1966809		37%	NT	NT	NT
247	SR-01000677508-2	92709283	1914729		18%	NT	NT	NT

Green highlight: active
NT: not tested

Table S2. Enzyme Names and Identifiers for ABPP-SILAC experiments

Abbreviation	Name	GeneID	Protein GI	Organism
Aadacl1 (Kiaa1363; Nceh1)	neutral cholesterol ester hydrolase 1	320024	30520239	<i>Mus musculus</i>
		57552	68051721	<i>Homo sapiens</i>
Abhd10	abhydrolase domain containing protein 10	55347	8923001	<i>Homo sapiens</i>
Abhd12	abhydrolase domain containing protein 12	76192	159110817	<i>Mus musculus</i>
		26090	109689718	<i>Homo sapiens</i>
Abhd6	abhydrolase domain containing protein 6	66082	31560264	<i>Mus musculus</i>
		57406	189027141	<i>Homo sapiens</i>
Acot1	acyl-coenzyme A thioesterase 1	26897	6753550	<i>Mus musculus</i>
Acot2	acyl-coenzyme A thioesterase 2	171210	238624114	<i>Mus musculus</i>
Apeh	acylpeptide hydrolase	235606	19343726	<i>Mus musculus</i>
		327	23510451	<i>Homo sapiens</i>
Ctsa	lysosomal protective protein	5476	119395729	<i>Homo sapiens</i>
Dpp4	dipeptidyl peptidase 4	13482	6753674	<i>Mus musculus</i>
Dpp8	dipeptidyl peptidase 8	74388	31542571	<i>Mus musculus</i>
Dpp9	dipeptidyl peptidase 9	224897	255003757	<i>Mus musculus</i>
		91039	67460390	<i>Homo sapiens</i>
Esd	esterase D/formylglutathione hydrolase	13885	13937355	<i>Mus musculus</i>
		2098	33413400	<i>Homo sapiens</i>
Faah	fatty acid amide hydrolase	14073	123253900	<i>Mus musculus</i>
Fasn	fatty acid synthase	14104	93102409	<i>Mus musculus</i>
		2194	41872631	<i>Homo sapiens</i>
Lipe	hormone-sensitive lipase	16890	87239972	<i>Mus musculus</i>
Lypla1	lysophospholipase 1	18777	6678760	<i>Mus musculus</i>
		10434	5453722	<i>Homo sapiens</i>
Lypla2	lysophospholipase 2	26394	7242156	<i>Mus musculus</i>
		11313	9966764	<i>Homo sapiens</i>
Lyplal1	lysophospholipase-like 1	127018	20270341	<i>Homo sapiens</i>
Mgl1 (Magl)	monoacylglycerol lipase	11343	6005786	<i>Homo sapiens</i>
Pafah1b2	platelet-activating factor acetylhydrolase 1B subunit beta	18475	40254624	<i>Mus musculus</i>
Pafah1b3	platelet-activating factor acetylhydrolase 1B subunit gamma	18476	6679201	<i>Mus musculus</i>
Pafah2	platelet-activating factor acetylhydrolase 2	100163	225579137	<i>Mus musculus</i>
Pla2g4a	cytosolic phospholipase A2	5321	23943920	<i>Homo sapiens</i>
Pnpla6	patatin-like phospholipase domain containing protein 6	50767	170763472	<i>Mus musculus</i>
		10908	260656037	<i>Homo sapiens</i>
Pnpla7	patatin-like phospholipase domain containing protein 7	241274	225007615	<i>Mus musculus</i>
Ppme1 (Pme1)	protein phosphatase methylesterase 1	72590	30794138	<i>Mus musculus</i>
		51400	7706645	<i>Homo sapiens</i>
Prcp	proline carboxypeptidase	72461	33469015	<i>Mus musculus</i>
Prep	prolyl endopeptidase	19072	6755152	<i>Mus musculus</i>
		5550	41349456	<i>Homo sapiens</i>
Sec23ip	Sec23ip protein	207352	133777972	<i>Mus musculus</i>
Tpp2	tripeptidyl peptidase 2	22019	37194903	<i>Mus musculus</i>
		7174	119629464	<i>Homo sapiens</i>